



# **Anterior Vertebral Stapling for the Fusionless Correction of Scoliosis**

**An anatomical and biomechanical investigation**

**Master of Engineering Thesis**

**School of Engineering Systems, QUT**

**Submitted by**

**Dr MARK PERNELL SHILLINGTON B.Phty., M.B.B.S.**

**November 2008**

## **KEYWORDS**

Fusionless scoliosis surgery, spine biomechanics, thoracic spine, staples, shape memory alloy, strain, growth modulation, hemiepiphysiodesis, bovine vertebra, micro-computed tomography, endoscopy, thorascopic.

## ABSTRACT

Fusionless scoliosis surgery is an emerging treatment for idiopathic scoliosis as it offers theoretical advantages over current forms of treatment. Currently the treatment options for idiopathic scoliosis are observation, bracing and fusion. While brace treatment is non-invasive, and preserves the growth, motion, and function of the spine, it does not correct deformity and is only modestly successful in preventing curve progression. In adolescents who fail brace treatment, surgical treatment with an instrumented spinal fusion usually results in better deformity correction but is associated with substantially greater risk. Furthermore in younger patients requiring surgical treatment, fusion procedures are known to adversely effect the future growth of the chest and spine. Fusionless treatments have been developed to allow effective surgical treatment of patients with idiopathic scoliosis who are too young for fusion procedures. Anterior vertebral stapling is one such fusionless treatment which aims to modulate the growth of vertebra to allow correction of scoliosis whilst maintaining normal spinal motion

The Mater Misericordiae Hospital in Brisbane has begun to use anterior vertebral stapling to treat patients with idiopathic scoliosis who are too young for fusion procedures. Currently the only staple approved for clinical use is manufactured by Medtronic Sofamor Danek (Memphis, TN). This thesis explains the biomechanical and anatomical changes that occur following anterior vertebral staple insertion using in vitro experiments performed on an immature bovine model. Currently there is a paucity of published information about anterior vertebral stapling so it is hoped that this project will provide information that will aid in our understanding of the clinical effects of staple insertion.

The aims of this experimental study were threefold. The first phase was designed to determine the changes in the bending stiffness of the spine following staple insertion. The second phase was designed to measure the forces experienced by the staple during spinal movements. The third and final phase of testing was designed to describe the structural changes that occur to a vertebra as a consequence of staple insertion.

The first phase of testing utilised a displacement controlled testing robot to compare the change in stiffness of a single spinal motion segment following staple insertion for the three basic spinal motions of flexion-extension, lateral bending, and axial rotation. For the second phase of testing strain gauges were attached to staples and used to measure staple forces during spinal movement. In the third and final phase the staples were removed and a testing specimen underwent micro-computed tomography (CT) scanning to describe the anatomical changes that occur following staple insertion.

The displacement controlled testing showed that there was a significant decrease in bending stiffness in flexion, extension, lateral bending away from the staple, and axial rotation away from the staple following staple insertion. The strain gauge measurements showed that the greatest staple forces occurred in flexion and the least in extension. In addition, a reduction in the baseline staple compressive force was seen with successive loading cycles. Micro-CT scanning demonstrated that significant damage to the vertebral body and endplate occurred as a consequence of staple insertion.

The clinical implications of this study are significant. Based on the findings of this project it is likely that the clinical effect of the anterior vertebral staple evaluated in this project is a consequence of growth plate damage (also called hemiepiphysiodesis) causing a partial growth arrest of the vertebra rather than simply compression of the growth plate. The surgical creation of a unilateral growth arrest is a well established treatment used in the management of congenital scoliosis but has not previously been considered for use in idiopathic scoliosis.

## TABLE OF CONTENTS

Chapter	Page
List of key words	2
Abstract	3
Table of illustrations and diagrams	7
Statement of original authorship	11
Acknowledgements	12
1. Clinical Problem and Study Aims	13
2. Literature Review	21
2.1 Vertebral anatomy and growth modulation	21
2.2 Anterior vertebral stapling	26
2.2.1 Animal studies of anterior vertebral stapling	26
2.2.2 Clinical results of anterior vertebral stapling	30
2.2.3 Aspects of staple design	31
2.2.4 Thoroscopic approaches to spinal surgery	34
2.3 Biomechanical testing of anterior vertebral stapling	35
2.3.1 Results of biomechanical testing	35
2.3.2 The use of calf spine models	36
2.3.3 Load vs. displacement controlled testing	38

3. Materials and Methods	41
3.1 Displacement controlled testing	42
3.2 Measurement of staple loading during spinal movement	47
3.3 Vertebral structural change following staple insertion	50
4. Results	51
4.1 Displacement controlled testing	51
4.2 Measurement of staple loading	57
4.3 Changes in vertebral structure following staple insertion	59
5. Discussion and Conclusions	61
References	67
Appendix 1: The effect of temperature on staple stiffness	74
Appendix 2: Post-test x-rays confirming staple position	77

## TABLE OF ILLUSTRATIONS AND DIAGRAMS

<b>Figures</b>	<b>Page</b>
1. Scoliosis deformity	13
2. (a) Coronal plane radiograph demonstrating a scoliosis, and (b) Schematic drawing illustrating the measurement of a Cobb angle.	14 14
3. Cervicothoracolumbosacral orthosis (CTLSSO).	15
4. Radiographs demonstrating a thoracic fusion procedure.	16
5. (a) The shape memory alloy (SMA) staple, and (b) Demonstration of staple insertion via thoroscopic technique.	18 18
6. (a) Intra-operative photos of staple insertion, and (b) Post-operative radiographs.	19 19
7. Schematic diagram showing the anatomy of a growing vertebra in the coronal plane.	22
8. Schematic demonstration of physeal stapling to correct angular deformity of the tibia in Blount's disease.	23
9. The concept of a "vicious cycle".	24
10. Radiograph demonstrating the creation of an experimental scoliosis in a goat using an asymmetrical rigid spinal tether.	25
11. Post-operative radiograph from Nachlas and Borden showing a staple inserted into a dog spine.	26
12. Radiographs demonstrating the creation of an experimental scoliosis in a goat.	27
13. (a) and (b), two alternative proposed staple designs.	29

<b>14.</b> Schematic drawing showing the tool used for intra-operative templating to determine staple size.	33
<b>15.</b> Intra-operative photograph demonstrating the thorascopic approach.	34
<b>16.</b> Schematic diagram representing (a) load-controlled compared to (b) displacement-controlled testing.	39
<b>17.</b> A functional spinal unit following preparation for testing.	42
<b>18.</b> The testing robot.	43
<b>19.</b> (a) The testing specimen fixed to the base plate, and (b) coupled to the testing apparatus.	44
<b>20.</b> Schematic diagram illustrating staple position in the spine.	46
<b>21.</b> Insertion of the SMA staple during testing.	46
<b>22.</b> Post- test radiograph confirming staple position.	46
<b>23.</b> (a) SMA staple with a strain gauge attached, and (b) set-up prior to testing, and (c) strain gauge connected to data logger.	48
<b>24.</b> Definition of equivalent staple tip force.	49
<b>25.</b> Staple tip force calibration for two of the strain gauged staples used in the testing.	50
<b>26.</b> Representative load-displacement graph for flexion-extension in the (a) control, and (b) stapled conditions.	54
<b>27.</b> Representative load-displacement graph for lateral bending in (a) control, and (b) staple conditions	55
<b>28.</b> Representative load-displacement graph for axial rotation in (a) control, and (b) staple conditions.	56
<b>29.</b> Time based plot of staple tip forces in flexion – extension.	57

<b>30.</b> Time based plot of staple tip force in lateral bending.	58
<b>31.</b> Time base plot of staple tip loading in axial rotation.	58
<b>32.</b> Coronal plane reconstruction of micro-CT.	60
<b>33.</b> Axial reconstruction of the micro-CT.	60
<b>34.</b> Photograph of an SMA staple.	66

<b>Tables</b>	<b>Page</b>
1. Ranges of motion used for testing and order of tests.	45
2. Results of paired t-tests comparing the stiffness of non-stapled and stapled motion segments.	52
3. Mean, minimum, maximum, and median stiffness values for each direction of movement in the control and stapled conditions (Nm/°).	53

**Statement of Original Authorship**

*The work contained in this thesis has not been previously submitted to meet requirements for an award at this or any other higher education institution. To the best of my knowledge and belief, the thesis contains no material previously published or written by another person except where due reference is made.*

A handwritten signature in black ink, consisting of several overlapping, fluid strokes that form a stylized, abstract shape.

Mark P Shillington, 12<sup>th</sup> November, 2008.

## **ACKNOWLEDGEMENTS**

To Clayton Adam, without whom this project would not have been possible. Your patience, approachable nature, and guidance inspired me to achieve new goals that would not have been possible without your help. Thanks for being contactable and always available and willing to help. Working with you has taught me many new skills and inspired an enthusiasm for research that I know will make me a better doctor.

To Geoffrey Askin and Robert Labrom, thank you for providing me with the wonderful opportunities that this job has given me. Having two experienced paediatric spinal surgeons who are friendly and encouraging as my mentors has been invaluable for my development.

Maree Izatt, thanks for always being welcoming and obliging, and for always providing me assistance with a smile. Your ability to provide information, pictures, articles, and technical advice, often at very short notice, was much appreciated.

Helen Cunningham, thanks for your help with learning the in's and out's of George and with the staple strain gauge testing. I really appreciated your generosity with your time when you had more than enough things on your plate!

Rob McPhee and National Surgical, thank-you for providing the staples for testing and the equipment required for their use.

Kristen Gilshenan, thank-you so much for your help with the statistics.

Brendon Evans, thanks for your assistance with the staple stiffness tests.

Last, but not least, thanks to my wife Rhiannon whose loving support allows me to be the best person I can be every day.

## CHAPTER 1. CLINICAL PROBLEM AND STUDY AIMS

This chapter describes the clinical problems associated with current treatment methods for scoliosis, and details the aims and objectives of this study.

Scoliosis, simply defined as lateral curvature of the spine, has been recognised clinically for centuries. The first descriptions of this condition were seen in ancient Hindu religious literature (circa 3500-1800 BC) where the treatment of spinal deformity was clearly described.<sup>58</sup> Over time our understanding of this condition has increased significantly yet many aspects of the condition still remain not fully understood. It is now recognised that the original descriptions of scoliosis as purely a lateral curvature of the spine were oversimplified, and rather the condition involves a complex three-dimensional deformity of the spine (Figure 1).<sup>99</sup> For practical purposes, however, the curvature is conventionally described and measured in one plane using standing coronal plane radiographs and the Cobb technique (Figure 2).<sup>28</sup>

This figure is not available online.  
Please consult the hardcopy thesis  
available from the QUT Library

**Figure 1.** Scoliosis deformity<sup>99</sup>

This figure is not available online.  
Please consult the hardcopy thesis  
available from the QUT Library

(a)

(b)

**Figure 2.** (a) Coronal plane radiograph demonstrating a scoliosis, and (b) schematic drawing illustrating the measurement of a Cobb angle.<sup>98</sup>

Paediatric spinal deformities such as scoliosis may result from many causes including neuromuscular disorders, congenital abnormalities, neurofibromatosis, connective tissue disorders, and skeletal dysplasia, however, in the majority of cases the cause is unknown, with this group referred to as idiopathic scoliosis. The aetiology of idiopathic scoliosis is incompletely understood but both genetic<sup>70</sup> and environmental<sup>44</sup> factors are thought to be involved. The prevalence rate of idiopathic scoliosis is approximately two percent with females having a far higher incidence than males.<sup>55,111</sup>

Based on the observation of three distinct peak periods of onset, patients with idiopathic scoliosis have been sub-divided into three groups based on the age at which they are diagnosed; (1) infantile, onset before age three years; (2) juvenile, age three to ten years; and (3) adolescent, age ten years until the end of growth.<sup>54</sup> Eighty percent or more of idiopathic scoliosis is of the adolescent variety.<sup>85</sup>

When making decisions about the treatment of patients with idiopathic scoliosis one of the primary considerations is the likelihood of the curve progressing in size. The natural history of curve progression is dependent on the patient's skeletal maturity, the curve pattern, and the curve severity.<sup>6,14,23,61</sup> Thus patients with significant growth potential and/or large curves at presentation are more likely to progress without treatment.

Until recently, the options for treatment of progressive scoliosis in a growing child were limited to observation, bracing, and surgery.<sup>61,111</sup> In patients with curves measuring 20 to 40 degrees the current standard of care is bracing with a cervicothoracolumbosacral orthosis (CTLSO) (see Figure 3) or a thoracolumbosacral orthosis (TLSO). Current reports show only modest results for this treatment, with 18 to 50 percent of treated curves progressing despite bracing.<sup>2,56,61,71,82,90,111</sup> In addition brace wear can be associated with many other problems including concerns about the effects of sustained pressure on the growing chest wall and the psychological impact related to the stigmata of having to wear a brace, especially in children who have to wear the brace for many years.<sup>3,7,26,27,37,56,60,64,75</sup> Also, while brace treatment is non-invasive and preserves the growth, motion, and function of the spine, it does not correct an established deformity of the spine. While most orthopaedic surgeons, families, and patients agree that it is reasonable to wear a scoliosis brace for one or two years if it means preventing an operation, a more difficult situation is encountered in the very young child who faces the prospect of wearing a brace for many years with no guarantee of a favourable outcome.

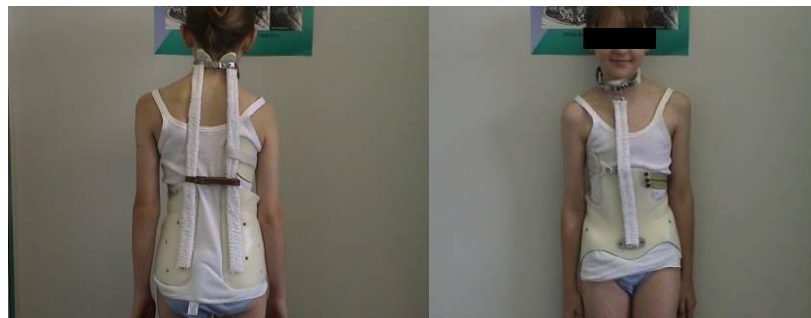


**Figure 3.** Cervicothoracolumbosacral orthosis (CTLSO)

For growing children that fail brace treatment or have more severe scoliosis, surgery is often considered. Operative treatment consists of spinal instrumentation with or without vertebral fusion. It may be carried out via a posterior, anterior (as shown in Figure 4) or combined approach. Although an instrumented spinal fusion provides better deformity correction than brace treatment, it is more invasive and carries more risk. Spinal instrumentation procedures, whether anterior or posterior, require extensive surgical dissection to expose the spine and prepare for fusion. The instantaneous correction of spinal deformity achieved during an instrumented spinal fusion procedure also carries the risk of neurologic injury. In addition, even with safe correction of scoliosis and a solid fusion, the growth, motion, and function of the fused portion of the spine are eliminated, perhaps increasing the risk of adjacent segment degeneration and spinal imbalance problems in the future.



**Figure 4.** Radiographs demonstrating an anterior thoracic fusion procedure

To address this clinical problem, new ‘fusionless’ treatment options are being developed. There are many synonyms for fusionless scoliosis surgery, including anterior or endoscopic vertebral stapling, convex scoliosis tethering, mechanical modulation of spinal growth, guided spinal growth, and even internal bracing of spinal deformity. Regardless of the name or implant applied to this unique method of treatment, the goal remains the same: to harness the inherent spinal growth of the patient with scoliosis and redirect it to achieve correction of the deformity. Like bracing, the fusionless treatment of scoliosis aims to preserve the growth, motion, and function of the spine but is also potentially more mechanically advantageous as corrective forces are applied directly at the spine rather than via the chest wall and ribs. Furthermore, unlike with bracing, the effectiveness of these treatments is not dependent on patient compliance. Like other surgical options, fusionless treatments are invasive, but less so with no requirement for extensive dissection of tissue. In addition, the neurological risk associated with instantaneous correction of deformity using rigid instrumentation may be lessened in fusionless surgery. Furthermore, the preservation of spinal motion and function may protect adjacent segments from premature degeneration over time.

Anterior vertebral stapling is becoming an increasingly popular fusionless treatment technique for young patients with idiopathic scoliosis who require surgical treatment. Currently the only staple with Therapeutic Goods Administration (TGA) and Food and Drug Administration (FDA) approval specifically for use in the anterior spine is the “Shape Memory Alloy Staple” (SMA)<sup>1</sup> which is manufactured by Medtronic. This staple is inserted via a thorascopic approach into the convex side of a scoliosis curve and spans adjacent vertebral endplates and discs (see Figures 5 and 6). It is believed that the staples act as a mechanical tether across adjacent vertebral growth plates on the convexity of the curve thus slowing growth and allowing deformity correction as the spine grows.

---

<sup>1</sup> See Section 2.2.3 on page 31 for further explanation of shape memory alloys and their use in staple design.

This figure is not available online.  
Please consult the hardcopy thesis  
available from the QUT Library

**Figure 5.** (a) The Medtronic SMA staple and (b) demonstration of  
insertion via thorascopic technique<sup>67</sup>



(a)



(b)

**Figure 6.** (a) Intra-operative photos of staple insertion and (b) post-operative radiographs

Despite the increasing clinical and academic interest in SMA staples, little is known about the anatomical effects of staple insertion on the vertebrae or the biomechanical consequences of their insertion on the spine. Accordingly, this study aims to investigate the consequences of SMA stapling in the thoracic spine to advance the understanding of this new treatment. Specifically, the objectives of the study are;

1. To experimentally determine the changes in bending stiffness of the thoracic spine in flexion, extension, lateral bending, and axial rotation following insertion of an SMA staple using a bovine model.
2. To measure and describe the forces which are placed on staples during spinal movements.
3. To describe the anatomical changes in vertebral structure associated with staple insertion.

## CHAPTER 2. LITERATURE REVIEW

This chapter describes literature relevant to the use of anterior vertebral staples to correct adolescent idiopathic scoliosis.

### 2.1 Vertebral anatomy and growth modulation

Beginning in childhood, vertebrae grow through thin growth plates on the superior and inferior vertebral end-plates and from the neuro-central, articular process and spinous process synchondroses (see Figure 7).<sup>11,12,111</sup> There is broad agreement that the anatomical abnormalities seen in the vertebrae of patients with scoliosis, which include vertebral wedging, disproportionate anterior spinal overgrowth, and intra-vertebral rotation, suggest that asymmetrical vertebral growth has occurred.<sup>13,34,45,46,79,80,88,97</sup> All types of scoliosis progress faster following the pubescent growth spurt, indicating that the shape of the vertebral body changes most rapidly with vertebral growth.<sup>62,112</sup> Therefore, because scoliosis progresses during the pubescent growth spurt, it is likely that the vertebral body growth plate is a major factor in the development of the scoliosis deformity. It was from this background information that the SMA staple was developed. Anterior vertebral stapling is proposed to have its effect by controlling the growth of the vertebral growth plate and thus correcting, or at least minimising, progression of the deformity.

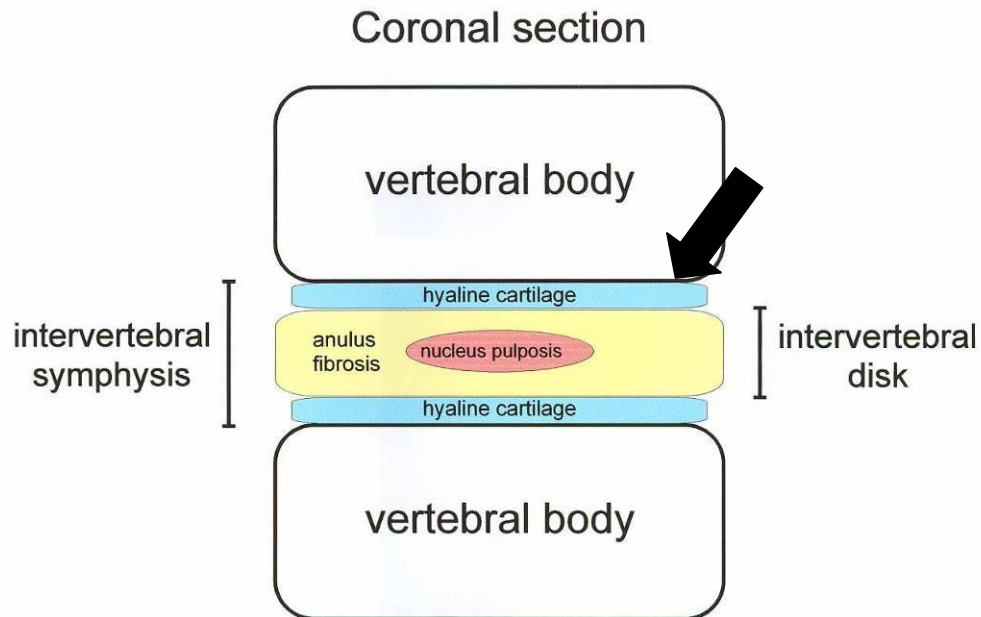


**Figure 7.** Schematic diagram showing the anatomy of a growing vertebra in the coronal plane. The block arrow indicates the location of the growth plate between the vertebral body and the hyaline cartilage end plate

The concept of growth modulation through mechanical tethering of the growth plate is well accepted for treating angular deformity of long bones in children (genu varum, genu valgum). This technique was pioneered by W.P. Blount in the late 1940's when stapling of the tibial physis for the correction of angular deformity was introduced.<sup>15</sup> In Blount's disease (tibia vara), the medial aspect of the proximal tibial physis grows slowly. Therefore, treatment is directed at restricting lateral tibial physeal growth. Staples across the physis limit growth asymmetrically, allowing deformity correction with continued growth of the unrestricted medial side of the growth plate (Figure 8). This experience with long bones provides a background rationale for attempting growth modulation in the deformed vertebral bodies of the scoliotic spine.

This figure is not available online.  
Please consult the hardcopy thesis  
available from the QUT Library

**Figure 8.** Schematic demonstration of physeal stapling to correct angular deformity of the tibia in Blount's disease. <sup>106</sup>

Although the aetiology of idiopathic scoliosis is poorly understood, it is thought that mechanical factors play an important role in the progression of the deformity during growth. <sup>4,16,32,41,66,81,86,95,118</sup> More specifically, the progression of vertebral wedge deformities is thought to be governed by the Hueter-Volkman law. <sup>5,52,68,69,100,101,108</sup> Under this law, growth plates subjected to increased compressive forces will demonstrate reduced growth, while those subjected to increased distractive forces will demonstrate accelerated growth. The 'vicious cycle' established by this growth differential is thought to contribute to the progression of scoliosis deformity (Figure 9). <sup>102</sup>

This figure is not available online.  
Please consult the hardcopy thesis  
available from the QUT Library

**Figure 9.** The concept of a “vicious cycle,” whereby spinal curvature increases during growth because it leads to asymmetric loading of vertebrae, which in turn causes asymmetric growth and additional wedging of the vertebrae.<sup>100</sup>

Using a rat-tail model Stokes et al demonstrated that mechanical modulation of vertebral growth could be predicted by the Hueter-Volkman law.<sup>101</sup> With the application of an external fixator to rat-tail vertebral segments, symmetric compressive axial loads reduced growth to 68% of controls, whereas symmetric tensile axial loads augmented growth to 114% of controls. Subsequent studies of asymmetric loads applied to vertebral segments in a rat-tail not only resulted in differential growth but also allowed for the creation and correction of vertebral wedge deformities.<sup>68,69</sup>

Although Stokes et al<sup>101</sup> laid the groundwork for additional studies of mechanical modulation of growth in the vertebrae, the rat-tail model did not provide adequate approximation of the anatomy and function of the human spine. The rat-tail model is ideal for an isolated study of growth modulation in a single vertebra, however, the methods and fixators used in this model are not directly applicable to scoliosis. To better understand the mechanics of growth modulation in scoliosis, larger animal models, approximating the size of a juvenile human, have been undertaken.

Growth modulation via the Hueter-Volkman effect has been demonstrated in a number of large animal studies in calf <sup>73,74</sup>, pig <sup>25,110,113</sup>, and goat <sup>18-20,22,92</sup> models. Each of these studies used either an asymmetrical rigid spinal tether (see Figure 10), rib resection, or a vertebral stapling or plating procedure to create asymmetrical loading on the vertebral growth plate and achieve growth modulation of vertebral growth.

This figure is not available online.  
Please consult the hardcopy thesis  
available from the QUT Library

**Figure 10.** Radiograph demonstrating the creation of an experimental scoliosis in a goat using an asymmetrical rigid spinal tether. <sup>17</sup>

## 2.2 Anterior vertebral stapling

### 2.2.1 Animal studies of anterior vertebral stapling

The earliest studies of fusionless scoliosis surgery in an animal model began more than 50 years ago when Nachlas and Borden pilot tested an anterior lumbar staple in a dog model.<sup>72</sup> The application of a stainless steel staple to the anterior lumbar spine, spanning multiple vertebral motion segments, was used to create a mild scoliosis deformity. However, the curves created were likely “sciatic” scoliosis, rather than structural deformities, as the posterior implantation of an anterior lumbar staple probably crimps the exiting nerve roots, causing unilateral pain and paraspinal muscle spasm. Correction of these curves, perhaps by the same mechanism, was described after the application of the staple to the opposite side of the lumbar spine. Although no measurements or data were provided on the six animals in the study, multiple radiographs were included. All the radiographs reveal a thin staple tenuously spanning two to three lumbar motion segments with multiple examples of staple mal-position, dislodgement, and even breakage (see Figure 11). Analysis of the information provided in this study does not justify the optimistic conclusions of the authors in support of this form of treatment. Following this early work, animal testing of vertebral staples was largely abandoned.

This figure is not available online.  
Please consult the hardcopy thesis  
available from the QUT Library

**Figure 11.** Post-operative radiograph from Nachlas and Borden showing a staple inserted into a dog spine.<sup>72</sup>

With recent renewed interest in the clinical use of stapling procedures several investigators have investigated the efficacy of vertebral stapling in large animal models. Braun et al <sup>21</sup> created an experimental scoliosis in goats using an asymmetrical spinal tether and then randomised the goats to several treatment groups (Figure 12). Of interest were two groups, one of which had the tether removed and an SMA staple inserted into the convexity of their curve, and another, which was created as the control group, had the tether removed but no staple inserted. In the staple group there was a statistically significant decrease in the magnitude of the curve at the end of the six to fourteen week treatment period. Conversely, in the control group, despite a decrease in curve size, the difference was not significant. Despite this, the overall improvement in curve magnitude was not significantly different between the two groups. In a similar paper in 2005 Braun et al <sup>17</sup> re-created the same experimental model, however, in contrast to their previous paper, they left the spinal tether in place and inserted the staples on the convexity of the curve. In these goats the average curve magnitude progressed from 77.3 degrees prior to staple insertion to 94.3 degrees after the treatment period. The results of this study have limited clinical relevance as these curves were large and rapidly progressive and would not be clinically deemed suitable for fusionless treatments.

This figure is not available online.  
Please consult the hardcopy thesis  
available from the QUT Library

**Figure 12.** Radiographs demonstrating the creation of an experimental scoliosis in a goat, then subsequent correction following removal of the tether and insertion of SMA staples. <sup>21</sup>

Two alternative staple designs have been evaluated in studies using porcine<sup>25,110</sup> and rat<sup>93</sup> models. These staples, which differ from the shape memory alloy staple evaluated in the aforementioned studies, consist of plate and screw components with the screws inserted parallel to the growth plate to anchor the plate component which then acts as a tether to growth (Figure 13). The authors have postulated that these staple designs would more effectively provide a uniform compression force across the growth plate when compared to the SMA staple thus providing a more favourable structure to reproduce the Hueter-Volkman effect. Both staple designs were able to create an increase in spinal curvature and vertebral wedging following insertion into a previously straight spine. A comparison study of the three staple designs is now needed.

This figure is not available online.  
Please consult the hardcopy thesis  
available from the QUT Library

**Figure 13.** (a) and (b) the two alternative  
proposed staple designs.<sup>25,93,110</sup>

### *2.2.2 Clinical results of anterior vertebral stapling*

The first reported use of anterior vertebral stapling in humans was by Nachlas and Borden in 1951.<sup>72</sup> Their reporting of the technique was positive however no results were provided. Three years later Smith and colleagues reported disappointing results following the stapling of human patients for congenital scoliosis.<sup>96</sup> Not surprisingly the scoliosis correction in these children was limited because they had little remaining growth when treatment was initiated and the curves were severe, with considerable rotational deformity. Some staples were noted to break or loosen, which was likely because the staples spanned several levels and were subjected to significant motion. Subsequent to this report anterior vertebral stapling seems to have largely been abandoned until recently when dissatisfaction with fusion techniques has renewed interest in fusionless modalities.

The first recent report of a patient series is that of Betz and colleagues, who published a retrospective review of the Philadelphia Shriners Hospital experience with SMA stapling in patients with adolescent idiopathic scoliosis.<sup>9</sup> This was a landmark study with promising results which revived clinical interest after the previously mentioned disappointing results with staples. Reported are the results of 21 patients with a total of 27 stapled curves and a mean follow-up of 11 months (range 3-26 months). Conclusions were largely drawn from a group of ten patients with greater than one year follow-up (mean 22.6 months) and a pre-operative Cobb angle of less than 50°. Progression of the Cobb angle by  $\geq 6^\circ$  or beyond 50° was considered failure of treatment. Within this group 6 of 10 (60%) remained stable or improved and 4 (40%) progressed. No major complications were reported so it was concluded that the technique was feasible and safe.

In their subsequent paper in 2005 Betz et al presented further results of their cohort which had increased to 39 patients with a total of 52 stapled curves.<sup>8</sup> Stability in this paper was defined as an increase in the Cobb angle of  $\leq 10$  degrees at follow-up. For the group of patients who were 8 years or older, with a less than 50° preoperative curve, and a minimum of one year follow-up, curve stability was 87%. Significantly, in patients 8 years or older and with preoperative curves less than 30°, the group who are likely to have the strongest clinical indication for this procedure, curve stability was 100%. Major complications occurred in one patient (2.6%, diaphragmatic hernia) and minor complications in five patients (13%). Further follow-up results from this cohort are eagerly awaited.

### *2.2.3 Aspects of staple design*

Lack of success in the early reported use of vertebral stapling was likely due to both poor patient selection and sub-optimal staple design.<sup>72,96</sup> To address the issue of staple design Medtronic Sofamor Danek (Memphis, TN) has designed a specific staple using nitinol, a shape memory alloy, which has Therapeutic Goods Administration (TGA) and Food and Drug Administration (FDA) approval specifically for use in the anterior spine.

Shape memory alloys are unique materials that have highly elastic properties and are able to return to their austenite phase shape at room temperature after being bent to a different shape at a cooled temperature. This behaviour is the 'shape memory' effect as suggested by the name. There are many types of alloys that exhibit these traits including Cu-Al, Ni-Al, Cu-Al-Ni, CU-Zn, Sn, CU-Zn-Al, and Ni-Ti. The most common used and widely investigated type of SMA is nickel-titanium (Ni-Ti), or, nitinol as used in the staples in this study.

Although the medical use of SMA's is relatively new, the earliest reports of their development date back to the 1930's. The specific use of nitinol as an SMA, was first developed in 1963 by Buehler and colleagues at the United States Naval Ordinance Laboratories. They created an alloy consisting of 50% titanium and 50% nickel and found it to have unusual properties including high elasticity and a shape memory effect.<sup>50</sup> Subsequently the name nitinol was created by placing the letters together as Ni-Ti-NOL (Naval Ordinance Laboratory).

In the medical field nitinol is best known for its use in cardiovascular stents.<sup>10,30,48,49</sup> Extensive corrosion and biocompatibility experiments have been performed with nickel-titanium alloys.<sup>24,35,91,94,114</sup> These evaluations have shown that nitinol produces no cytotoxic, allergic, or genotoxic responses.

When nitinol is created with a 50:50 concentration of nickel and titanium the transition temperature is known to be approximately 30°. The transition temperature however can be manipulated by changing the alloy content, for instance if there is less nickel content the metal would have a higher transition temperature and vice versa. The precise transition temperature of the nitinol used to manufacture the vertebral staples used in this study has not been released by the manufacturer. On bench testing at our laboratory we have estimated it to be approximately 25°. This temperature is significantly lower than normal body temperature (normally 37.5°), however, to ensure that the staples are heated above their transition temperature following insertion it is likely that the manufacturer has chosen a lower temperature to allow a margin for variations in body temperature intra-operatively.

The manufacturing of these vertebral staples using a shape memory alloy allows the surgeon to alter the shape of the staple both prior to, and, following insertion into the patient's spine. Prior to insertion in the operating theatre the staple is placed in an ice bath to cool the nitinol below its transition temperature. Once this is achieved the surgeon is able to open the staple tines so that they are parallel with each other allowing accurate insertion with minimal trauma. Following insertion the staples are 'warmed' as they equilibrate with the patient's body temperature. This warming causes the staples to return to their original shape and thus 'clamp' down in position.

SMA staples are available in 2-prong and 4-prong variants, and come in sizes ranging from 4 to 14 millimetres. Currently the 4-prong staple is almost exclusively used with the use of two two prong staples per level occasionally reported. Staple size is chosen intra-operatively using templates and image intensification (see Figure 14).

This figure is not available online.  
Please consult the hardcopy thesis  
available from the QUT Library

**Figure 14.** Schematic drawing showing the tool used for intra-operative templating to determine staple size. The position of the tool is checked using image intensification.<sup>67</sup>

#### 2.2.4. Thorascopic approaches to spinal surgery

Anterior vertebral staples are inserted into the spine using video-assisted thorascopic surgery (VATS). In VATS the patient is positioned in a side-lying position, the upper lung is deflated and three small portals are created between the patient's ribs to allow access to the thoracic cavity and anterior vertebral bodies (see Figure 15). The use of this procedure was first described in 1993 for the treatment of vertebral body disease<sup>63</sup> and subsequently numerous authors have reported using VATS for anterior thoracic and thoracolumbar reconstruction, and, anterior release and fusion for the treatment of scoliosis.<sup>38,51,65,89</sup>

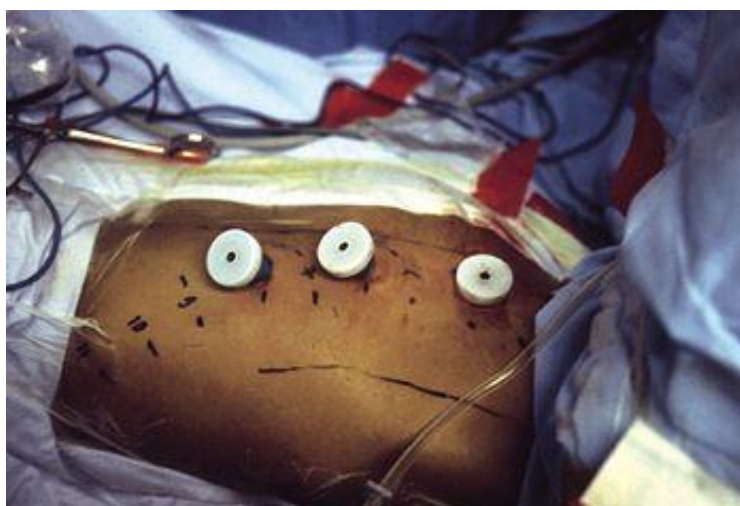


**Figure 15.** Intra-operative photograph demonstrating the thorascopic approach

In traditional scoliosis correction procedures, posterior instrumentation continues to be the gold standard, however according to recent literature anterior procedures may be more advantageous.<sup>40,47</sup> Proponents of anterior VATS techniques cite advantages including anatomic visualisation at least equivalent to, if not better than open thoracotomy, less trauma to the chest wall, less post-operative pain, shorter hospital stays, lower complication rates, quicker recovery rates, shorter rehabilitation, and possible decreased medical costs.<sup>31,53,59</sup>

## **2.3 Biomechanical testing of anterior vertebral stapling**

### *2.3.1 Results of biomechanical tests*

Despite the recent increased clinical and academic interest in the use of SMA staples, little is known about the biomechanical consequences of their insertion on the growing spine. Currently the only published information is that from Puttlitz and colleagues<sup>83</sup> who used a mature bovine spine model to measure changes in range of motion following staple insertion. In this study they used motion segments consisting of T4-T9 vertebrae which were initially subjected to non-destructive pure moment loading in an unstapled (control) condition. Following this, staples were inserted at three vertebral levels in a variety of positions including anterior, lateral, and combinations of both and the tests repeated. Range of motion was recorded using stereophotogrammetry and analysed using a custom-designed MATLAB program.

Following staple insertion a statistically significant decrease ( $p < 0.05$ ) in range of motion was reported in axial rotation and lateral bending, however, analysis of this result was difficult as no actual figures were given. There was no change in range of motion in flexion-extension following staple insertion. These results provide some guidance on the biomechanical changes associated with staple insertion, however they need to be interpreted with caution. The statistically significant results reported were of low power and where statistically significant results were reported to have been achieved absolute figures for the range of motion were not given. In addition, a custom designed testing apparatus was constructed for the purposes of the study, which may have been better served by the use of a validated testing technique. Furthermore, following each test staples were removed from testing specimens and the same specimen was subsequently re-used. In our experience staple removal is associated with significant damage to the vertebra and thus would confound results of further tests. Finally, mature bovine models, as used in this study, have few anatomical or physiological similarities to human spines.<sup>29,115,116</sup> A better experimental model may have been an immature (6-8 week old) bovine model which has been shown to be a good anatomical and physiological model for the human spine.<sup>29,104,115,116</sup> Nonetheless this paper provides a framework for much needed further investigations.

### *2.3.2 The use of calf spine models*

The use of animal models in biomechanical research is an accepted practice to reduce specimen cost, variation, and health risk. Calf spines are commonly substituted in experimental models and several publications have confirmed their validity as a substitute for cadaveric spines.<sup>29,84,115,116</sup>

Cotterill et al <sup>29</sup> undertook a comparative anatomical study between adult human and calf thoracolumbar spinal segments. They found that equivalent thoracolumbar vertebral lengths were obtained by selecting 6-8 week old calves. Differences in vertebral body parameters of width, length, height, and area were found at all levels, with the most similarities occurring at T6. In the thoracic spine the antero-posterior dimension was on average 56% larger in the bovine specimen ( $p>0.01$ ), however this difference was largely a result of the spinous process being 111% greater in length than that of a human. Furthermore thoracic spine measurements of lateral dimensions, transverse process shape and orientation, and facet joint orientation showed no significant difference.

Swartz et al <sup>104</sup> compared the physical and mechanical properties of calf and human lumbar trabecular bone. The mean tissue density, equivalent mineral density, apparent density, ash density, ash content, compressive strength, and compressive modulus of the calf spine were similar to a young human spine. The compressive strength of the calf spine increased from posterior, near the facet, to the anterior vertebral body, in contrast to the human. Human cadaveric specimens had a range of pathologies, including osteoporosis and disc and facet joint degeneration, that was not found in calf spines. Based on the physical and mechanical properties the authors concluded that the calf spine was a good model to represent a young, non-osteoporotic human spine.

Wilke et al <sup>115,116</sup> investigated and described the range of motion, neutral zone, and stiffness of thoracic and lumbar calf spines. The results were similar to those previously reported in the human spine and validated the use of calf spines as a model for human spines in biomechanical testing.

### 2.3.3 Load control versus displacement control testing

The human spine is a complex columnar structure made up of both active and passive elements. Due to this complexity the most desirable method for understanding the kinematics and kinetics of the human spine is through *in vivo* studies. *In vivo* studies do have inherent problems however when used as an experimental model. These problems are related to a number of factors that vary from patient to patient. These factors include variability in both the extent of injury and the corresponding extent of structural weakening for the particular condition evaluated, as well as variation in inhibition and/or facilitation of muscles (and thus changes in loads) to minimise pain and discomfort. Further confounding these variables are the changes in spine stiffness with age and the healing of tissue that occurs with time following surgery.

*In vitro* studies can provide a more objective assessment of the effect of an injury or surgical procedure on the spine because the involved variables can be more easily controlled. *In vitro* mechanical testing of the spine can be carried out in either a load-controlled or a displacement-controlled manner. Each method requires certain assumptions and offers different advantages.<sup>39,76</sup> In load controlled testing, a pure constant moment is incrementally applied to the spine and the spine is typically loaded in one plane at a time (i.e. flexion-extension, lateral bending, or axial rotation).<sup>36,77,78</sup> This means that the operator can precisely adjust the load and then measure the displacement that occurs as a result of the applied load. Under displacement control, the translational and rotational motions of the vertebrae rather than the load are controlled, with the load required to attain the desired motion measured (see Figure 16).<sup>1,42</sup> Both testing methods have inherent advantages and disadvantages and their relative superiority is frequently debated.

<sup>39,76</sup>

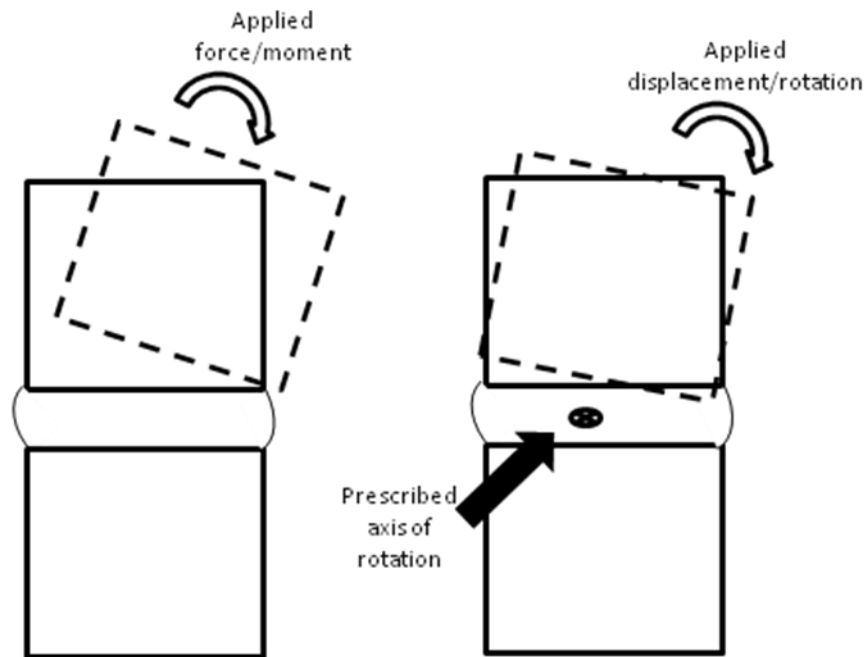


**Figure 16.** Schematic diagram representing (a) load-controlled compared to (b) displacement-controlled testing. In load-controlled testing a load and direction is set with the the motion segment moving freely in response to this load. In displacement-controlled testing the amount of displacement is set rather than the load, and the vertebrae rotate around a pre-determined, fixed axis of rotation (indicated by solid arrow).

The proposed advantages of load-controlled testing are that it allows constant loading at all levels of the testing specimen regardless of changes in function after injury or spinal instrumentation, and that (as occurs with *in vivo* conditions) load controlled testing allows the specimens to move freely in response to the external load. However those opposed to this form of testing cite that if load controlled tests are used to evaluate spinal implants, the specimen is likely to rotate around different centres of rotation after each intervention. This results in the remaining components of a joint producing a different resistance to the motion and hence the true comparative effect cannot be deduced.<sup>33</sup> A further disadvantage of this form of testing occur when testing specimens with low stiffness where large displacements can occur with little or no change in load making results difficult to interpret and potentially damaging testing specimens.

Displacement control is proposed to reveal the true relative affect of interventions to a component of a joint.<sup>33</sup> By ensuring all factors, including the motion path of the testing specimen, remain uniform displacement controlled testing may potentially allow greater validity and reliability when making comparisons pre- and post-insertion of a spinal implant. In addition, in low stiffness situations this form of testing allows for a more controlled testing environment. Conversely in high stiffness environments displacement control may be inappropriate because large changes in load can be produced by small changes in applied displacement. Those against this form of testing state it's major disadvantage as being that this form of testing poorly reflects the normal movement of the spine due to the complex forces imposed by simply displacing one end of the spine, thereby resulting in large, "unphysiological" coupled loads.<sup>43</sup> Those opposed to this argument propose that this affect can be minimised by maintaining primary deformations imposed on the specimen within physiological limits.<sup>33</sup>

### CHAPTER 3. MATERIALS AND METHODS

This chapter describes the experimental apparatus used to investigate the effects of SMA staple insertion on the vertebral column.

Immature bovine spines from six to eight week old calves, which have been shown to be a valid model for the adolescent human spine, were chosen as the experimental model.<sup>29,84,104,115,116</sup> These specimens were obtained from a local abattoir and stored frozen at the testing facility. Prior to testing all spines underwent computerised tomography (CT) scanning to exclude vertebral anomalies.

Each vertebral column was cut into monosegmental functional spinal units (FSU), consisting of two adjacent vertebrae with intervening discs, facets, and ligaments. The levels chosen were T3-4, T5-6, and T7-8, as these represent the levels most commonly treated in clinical practice. Using careful dissection each FSU was denuded of all paraspinal musculature with care to preserve the ligaments and bony structures. In addition, the ribs and a portion of the spinous process was removed. The latter was done to induce significant instability in the segment thus allowing sufficient range of motion within the segment for a comparison study. Three screws were placed in the superior and inferior end-plates of each testing specimen to ensure rigid fixation and the specimen was then potted in base plates using polymethylmethacrylate to facilitate coupling to the testing apparatus. (see Figures 17, 18, and 19). Each specimen underwent testing procedures of up to two hours duration so care was taken to ensure that results were not influenced by specimen dehydration. To avoid dehydration specimens were kept moist with water from a spray bottle, and whilst not actively testing, for example while cement was drying, were wrapped in a moist dressing.



**Figure 17.** A functional spinal unit following preparation for testing

SMA staples were obtained from the local distributor. The staples are available in both two and four-pronged designs however only a four pronged staple was used as this is the design currently used in clinical practice. A five millimetre staple size was chosen following templating from the pre-test CT scans.

To achieve the study aims three phases of testing were undertaken and are described below.

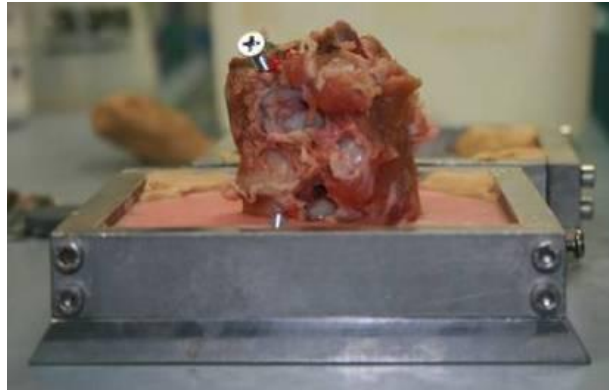
### *3.1 Displacement-controlled testing*

The first stage of testing was designed to measure changes in the bending stiffness of a single spinal motion segment following staple insertion.

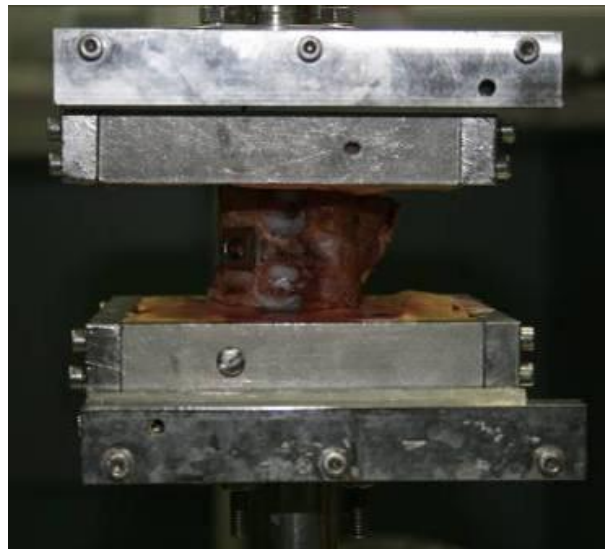
A custom-designed, six degree-of-freedom, displacement-controlled robotic facility was used as the testing apparatus (see Figure 18).<sup>33</sup> Potted specimens were attached to the mounting plates. Force and moment data for each test was recorded via the robot's force transducer at a sampling rate of approximately 20 hertz. A fixed axis of rotation for the segment was calculated to be five millimetres anterior to the posterior edge of the annulus in the mid-sagittal and mid-axial planes. Using a custom designed MATLAB program (version 6.0, MathWorks Inc., Natick, MA) the force transducer data was synchronised with the robot position data and filtered using moving average methods. The rotational stiffness of the motion segment for each applied motion was calculated as an average of five cycles per test, which were performed following one 'settling' cycle, and expressed in Nm/degree of rotation. For each motion, stiffness was calculated as the secant of the torque versus rotation curve between zero and the absolute maximum torque reached during the motion.



**Figure 18.** The testing robot



(a)



(b)

**Figure 19.** (a) The testing specimen fixed to the base plate and (b) coupled to the testing apparatus.

Fourteen tests were undertaken in order to achieve adequate statistical power. The vertebral levels used were six T3-4 segments, four T5-6 segments, and four T7-8 segments. Once prepared each specimen was first tested in a non-stapled (control) condition through a pre-determined range of motion firstly in flexion-extension, secondly in lateral bending, and finally in axial rotation (see Table 1). The range of motion values were obtained from normal values previously published by Wilke et al.<sup>115,116</sup> No axial load was applied to the specimen by the testing apparatus. The displacement rate was one degree per second for all tests.

**Table 1.** Ranges of motion used for testing and order of tests

Test order	Movement	Range of motion
1	Flexion → Extension	+2.5° → -1.5°
2	Lateral bending	+/- 3°
3	Axial rotation	+/- 4°

Following this an SMA staple was inserted into the left side of the motion segment and the test repeated. The staple was inserted according to the recommended operative technique supplied by the manufacturer.<sup>67</sup> This technique involved cooling the staple below its transition temperature in an ice bath, then ‘opening’ the staple to 90° using a custom designed tool. Following this the staples were inserted under direct vision just anterior to the insertion of the rib head so that they spanned the disc and the adjacent vertebral endplates (see Figures 20 and 21). Post-testing radiographs were used to confirm accurate staple placement (see Figure 22).

All tests were performed at room temperature. This was done because an additional experiment to evaluate the effect of heating the staple from room temperature (~23°) up to normal body temperature (~37°) resulted in only a small increase in stiffness from 52.6 N/mm to 56.7 N/mm, a change of less than 10% of the overall stiffness of the staple (see appendix 1). This small increase, despite being statistically significant, was likely to biomechanically make little difference to the overall results.

This figure is not available online.  
Please consult the hardcopy thesis  
available from the QUT Library

**Figure 20.** Schematic diagram illustrating staple position in the spine. Staples are inserted anterior to the rib heads and span adjacent vertebral endplates and the intervertebral disc.

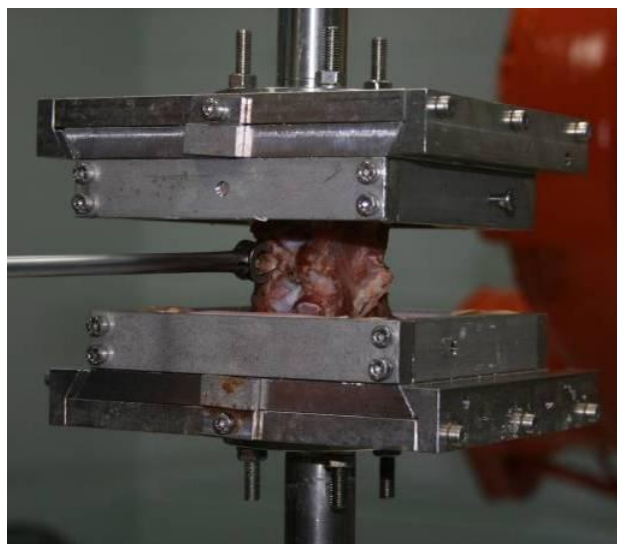


**Figure 21.** Insertion of the SMA staple

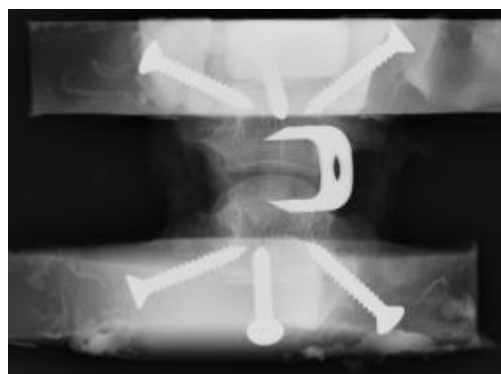


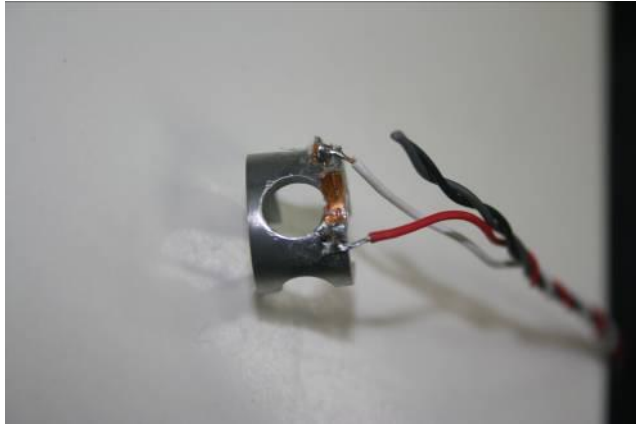
**Figure 22.** Post- test radiograph

Paired t-tests were used to compare average stiffness measurements in the stapled and control (no staple) conditions for each direction of movement. A significance level of  $p < 0.05$  was considered statistically significant.

### *3.2 Measurement of staple loading during spinal movement*

The second phase of testing was designed to investigate the forces on the staple during spinal movements. In addition, it was planned to use these results to quantify the force at the interface between the staple tips and the surrounding bone.

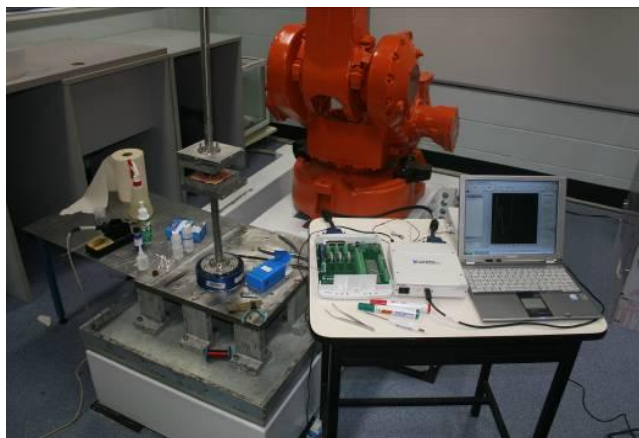
The testing apparatus and protocol for this phase of testing was identical to that described in phase one. Following insertion of the staple into the testing specimen a single axis  $120\Omega$  strain gauge (Vishay Micro-measurements, Singapore) was glued to the base of three of the staples in order to measure the forces experienced by the staple during the prescribed motions (see Figure 23).



(a)



(b)



(c)

**Figure 23.** (a) SMA staple with a strain gauge attached, (b) set up prior to testing, and (c) strain gauge connected to data logger.

Each specimen was then tested through the ranges of motion as described in phase one and strain data from the base of the staple was recorded on a data logger (National Instruments USB-6259, Austin, Tx). Following testing each strain-gauged staple was removed and individual calibrations were performed using a 1.5kN Hounsfield Universal Testing Machine (Tinius Olsen Ltd., Surrey, UK) to apply prescribed separating forces between the staple tips. Using this calibration data the staple strain data was converted into an equivalent staple 'tip' force in Newtons (defined as a force acting normal to, and positioned at the staple tips, with positive values tending to separate two opposing staple tips, and vice versa) (see Figure 24). Figure 25 shows the staple tip force calibration for two of the strain gauged staples used in the testing. The calibration varied slightly for each staple because of small variations in the positioning of the strain gauge.

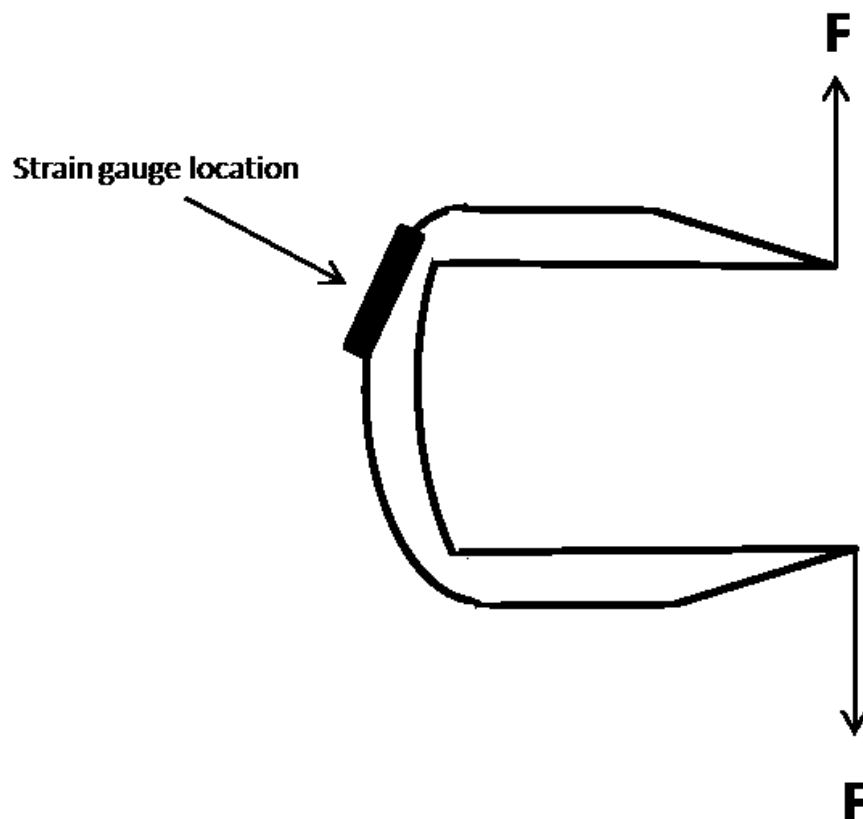


**Figure 24.** Definition of equivalent staple tip force,  $F$ .

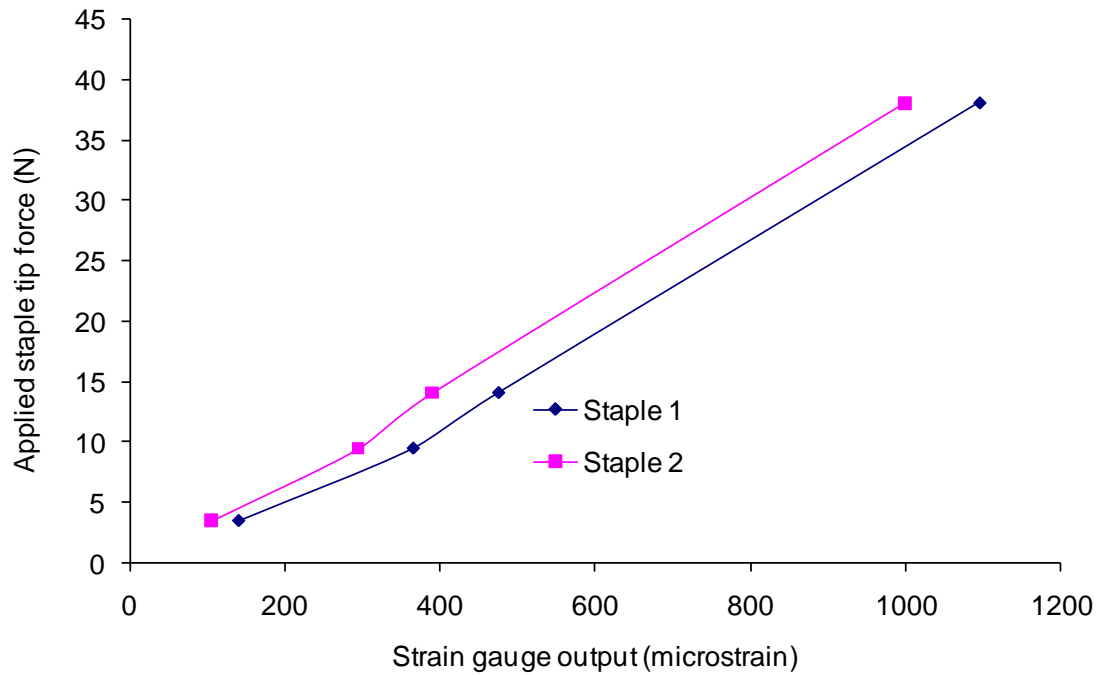


**Figure 25.** Staple tip force calibration for two of the strain gauged staples used in the testing.

### *3.3 Investigation of vertebral structural changes following staple insertion*

The final phase of testing was a descriptive study of the damage caused to the structural elements (that is the periosteum, trabecular bone, and growth plate) of the vertebra following insertion of an SMA staple. For this phase of testing a specimen that had completed phase one of the investigation were used. Micro-CT was only performed on one specimen as post-testing x-rays showed that staple position was consistent for all tests and thus it was expected that all micro-CT scans would show similar results (see appendix 2). Following completion of the phase one testing the specimen was carefully cut from the mounting pot. In order to minimise any additional vertebral damage caused by staple removal, a diamond saw (Microslice 2, Malvern Instruments, England) was then used to cut the staple in half. The two staple halves were then carefully removed from the vertebrae. The specimen subsequently underwent micro-CT scanning using a uCT-40 scanner (Scanco Ltd, Switzerland) at an isotropic voxel resolution of 36 microns. Image reconstructions were used to create a descriptive picture of the structural damage.

## CHAPTER 4. RESULTS.

### *4.1. Displacement controlled testing*

Stiffness measures in the non-stapled control group reflected the previously published results of Wilke et al.<sup>115,116</sup> The results of the comparison in motion segment bending stiffness between the stapled and non-stapled specimens are presented in Table 2.

A significant decrease in stiffness ( $p < 0.05$ ) following staple insertion was found in flexion, extension, lateral bending away from the staple, and axial rotation away from the staple. Stiffness for axial rotation towards the stapled side was significantly greater than for away. A near significant increase in lateral bend stiffness away from the staple compared with towards was also seen.

The mean, minimum, maximum, and median stiffness values for each direction of movement in both the control and stapled conditions is presented in Table 3. Note that the stiffness reduction with staple insertion is small, varying between 2% and 9% for the different motions tested.

Characteristic load-displacement graphs for each direction of movement are shown in Figures 26, 27, and 28.

**Table 2.** Results of paired t-tests comparing the stiffness of non-stapled and stapled motion segments

<b>Movement</b>	<b>Range of motion</b>	<b>Change in stiffness with staple insertion</b>	<b>P-value (*p&lt;0.05)</b>
Flexion	2.5°	↓	0.0003*
Extension	1.5°	↓	0.04*
Lateral bend towards staple	3°	-	0.09
Lateral bend away from staple	3°	↓	0.02*
Axial rotation towards staple	4°	-	0.25
Axial rotation away from staple	4°	↓	0.01*
Lateral bend toward staple vs. away	3°	-	0.06
Rotation toward staple vs. away	3°	↑ towards	0.04*

**Table 3.** Mean, minimum, maximum, and median stiffness values for each direction of movement in the control and stapled conditions (Nm/°). Standard deviation is included in brackets.

Movement	Mean			Minimum		Maximum		Median	
	Control	Staple	Change (%)	Control	Staple	Control	Staple	Control	Staple
Flexion	2.76 (0.44)	2.56 (0.37)	-7.25	2.05	1.84	3.53	3.10	2.70	2.53
Extension	2.56 (0.65)	2.41 (0.63)	-5.86	1.84	1.64	3.86	3.46	2.28	2.30
Lateral bend towards staple	2.31 (0.43)	2.26 (0.52)	-2.16	1.68	1.42	3.27	3.44	2.12	2.19
Lateral bend away from staple	2.51 (0.51)	2.37 (0.70)	-5.58	1.66	1.33	3.57	3.75	2.49	2.40
Axial rotation towards staple	0.34 (0.11)	0.33 (0.12)	-2.94	0.15	0.13	0.60	0.57	0.34	0.33
Axial rotation away from staple	0.33 (0.09)	0.30 (0.09)	-9.09	0.15	0.10	0.47	0.41	0.34	0.30

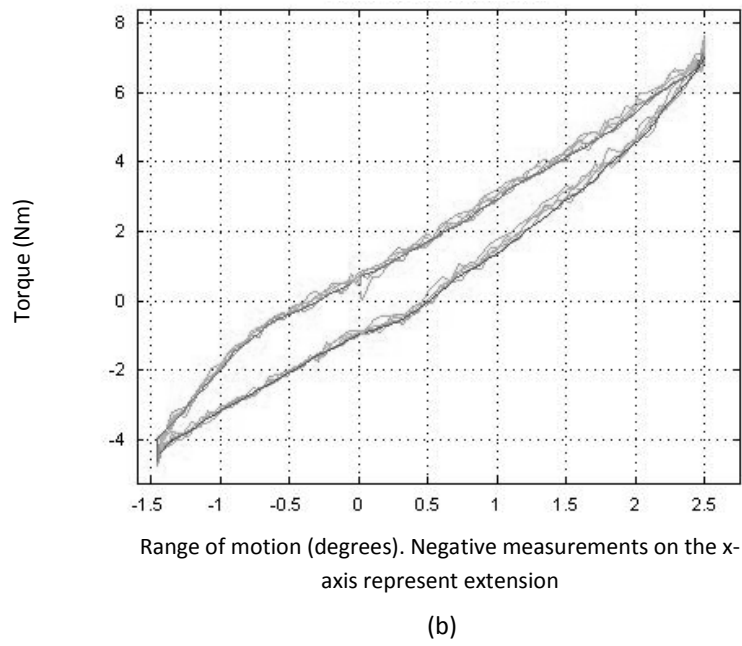
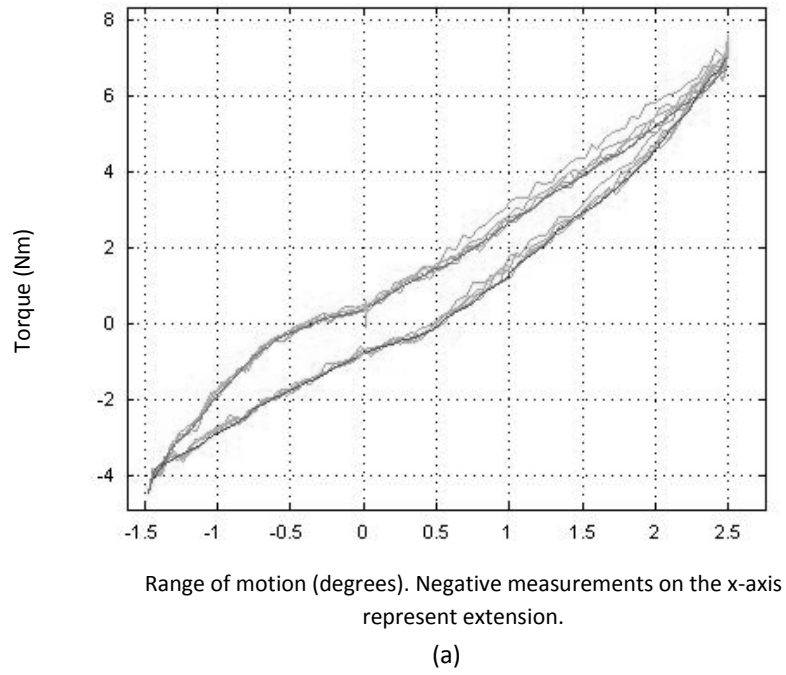
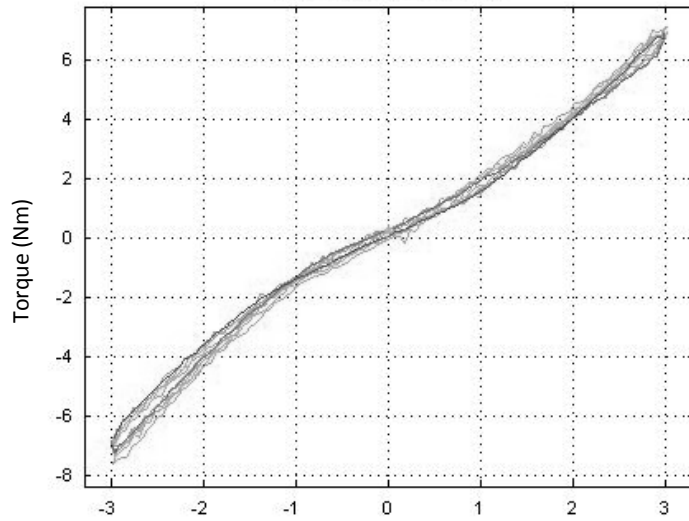
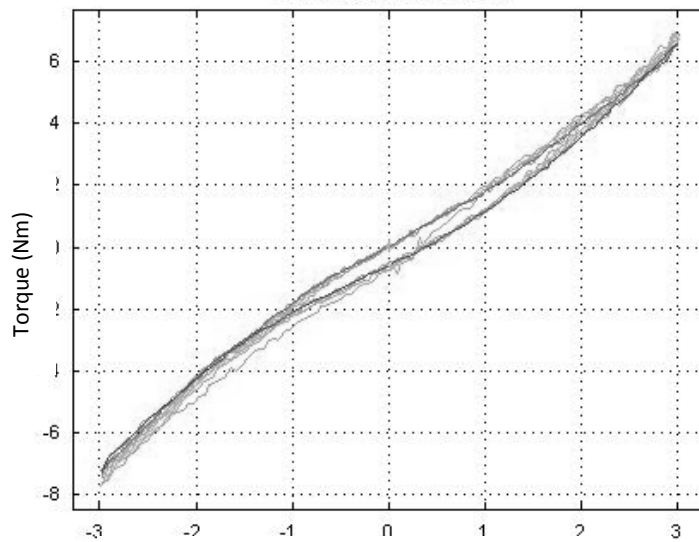


**Figure 26.** Representative load-displacement graph for flexion-extension in the (a) control, and (b) stapled conditions.



Range of motion (degrees). Negative measurements on the x-axis represent movement away from staple.

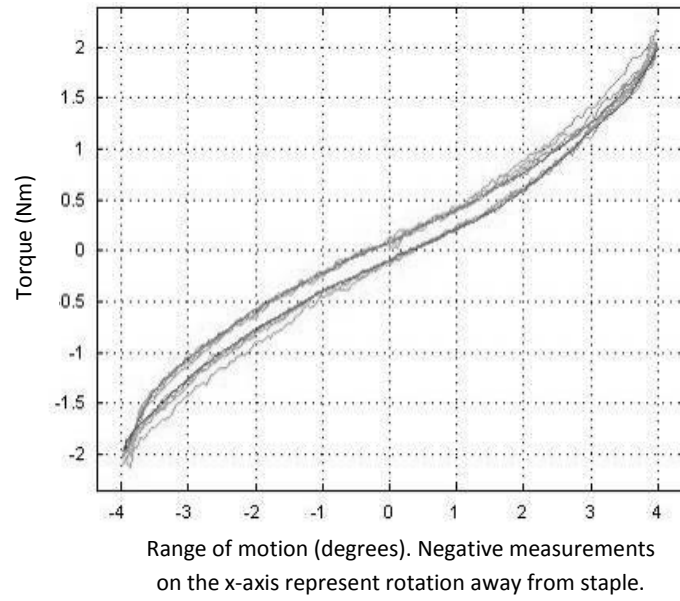
(a)



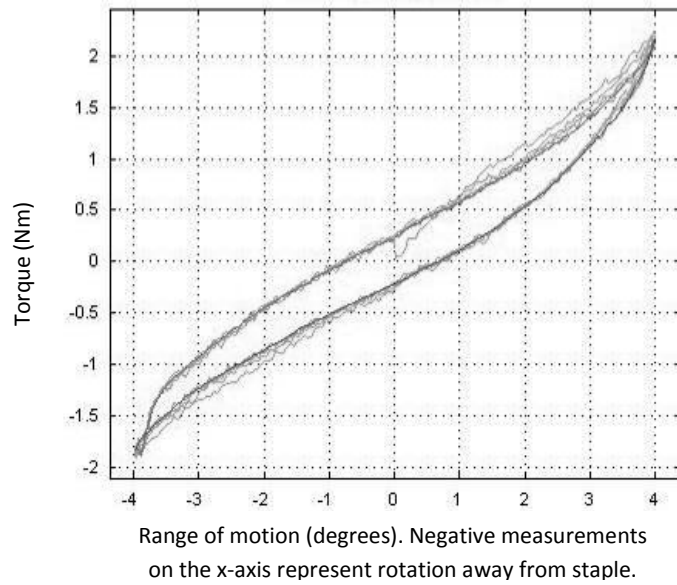
Range of motion (degrees). Negative measurements on the x-axis represent movement away from staple.

(b)

**Figure 27.** Representative load-displacement graph for lateral bending in (a) control, and (b) staple conditions



(a)



(b)

**Figure 28.** Representative load-displacement graph for axial rotation in the (a) control, and (b) stapled condition.

#### *4.2 Measurement of staple loading*

Representative selections of time-based plots of staple tip loading in each plane of motion are shown in Figures 29, 30 and 31. Following staple insertion a static or baseline compressive force at the staple tips is seen (demonstrated in figure 29). This is likely to have occurred due to the staple blades “clamping down” causing the staple to change shape as they are inserted into the vertebra and thus creating a baseline negative strain on the staple. During movement additional dynamic compression and tension forces are seen with the greatest dynamic force occurring in flexion and the least in extension. These dynamic forces are approximately symmetrical for lateral bending and rotation (i.e. the staple experiences a similar amount of compression then tension according to the direction of movement), however for flexion-extension strain is much greater in flexion than extension. This result is likely to be related to the relationship between the staple and the IAR for the specific plane of movement which is being tested, that is for lateral bending and rotation the staple position is such that it is loaded symmetrically about the fixed IAR for each plane of movement, but in flexion–extension the staple is not aligned with the coronal plane IAR and hence is loaded asymmetrically. Interestingly, across progressive testing cycles a gradual, but consistent, decrease in the base line compressive force is seen. This decrease is likely a consequence of trabecular bone fracture adjacent to the staple blades which occurs with motion segment movement (see discussion).

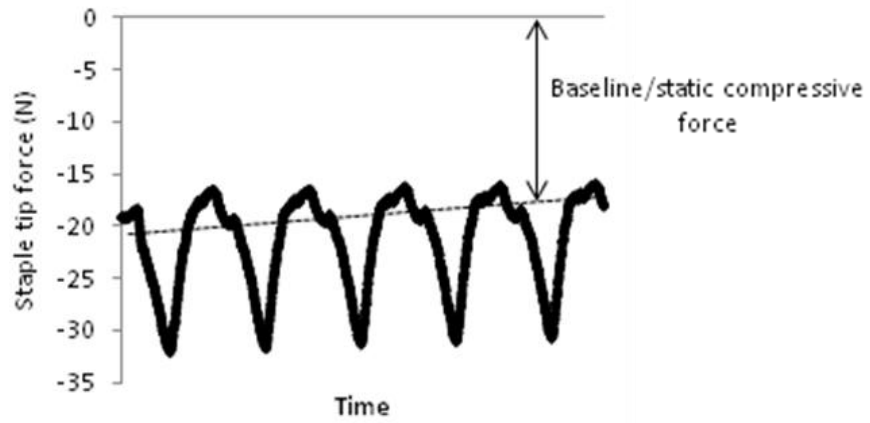


Figure 29. Time based plot of staple tip forces in flexion – extension.

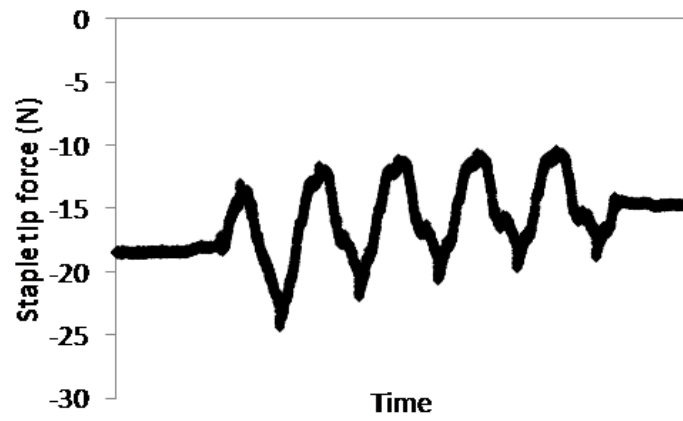


Figure 30. Time based plot of staple tip force in lateral bending

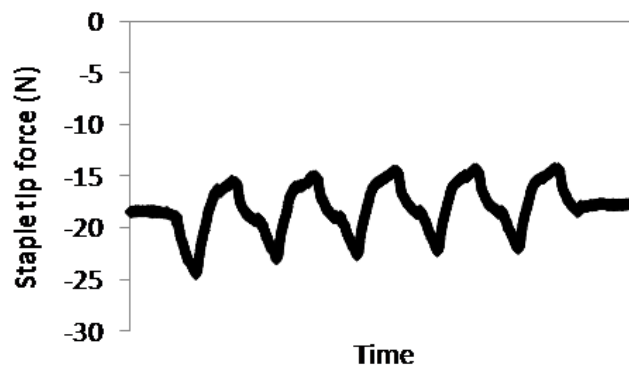


Figure 31. Time base plot of staple tip loading in axial rotation

#### *4.3 Changes in vertebral structure following staple insertion*

Micro-CT reconstructions of the scanned specimen are shown in Figures 32 and 33. The figures depict significant trabecular bone damage around the staple blades. In addition, unilateral destruction of the growth plate with penetration of the staple tips into the vertebral end-plate has occurred.

A further interesting finding depicted in the micro-CT scans is that the staple blades appear to have 'clamped' or closed down. The pattern of trabecular bone damage above the staple blades suggests that this clamping has occurred during insertion of the staple rather than, as would be expected with a shape memory alloy, following insertion when the staple should return to its original shape following heating above the transition temperature.



**Figure 32.** Coronal plane reconstruction of micro-CT demonstrating significant damage to one side the vertebral growth plate following staple insertion (indicated by arrow).



**Figure 33.** Axial reconstruction of the micro-CT showing significant trabecular bone damage (indicated by arrow) around the staple blades following staple insertion.

## CHAPTER 5. DISCUSSION.

The goal of this project was to describe the anatomical and biomechanical consequences of the insertion of an SMA staple in the thoracic spine. The findings from the biomechanical investigation indicate that staple insertion consistently decreased the stiffness of the motion segment. A statistically significant decrease was seen in flexion, extension, lateral bend away from the staple, and axial rotation away from the staple, furthermore, for lateral bend towards the staple and axial rotation towards the staple, despite not achieving statistical significance, the mean stiffness was decreased. These results could not be attributed to changes in anatomy or tissue properties between tests as each specimen acted as its own control.

Intuitively staple insertion would be expected to increase motion segment stiffness. Indeed, a recent paper by Puttlitz et al found a small but significant decrease in the range of motion in lateral bending and axial rotation using moment controlled testing.<sup>83</sup> In this paper T4-T9 motion segments were stapled with a variety of constructs and compared to a non-stapled control condition. The significance of these results were questionable however as the changes in range of motion were only a few degrees over several vertebral levels and statistical outcomes were of low power. Furthermore methodological flaws, in particular the fact the vertebrae were re-used for testing after removal of a staple which in our experience is associated with significant structural damage, make these small differences in range of motion difficult to interpret.

Aside from methodological issues another potential reason for the differing results between the results of this investigation and those of Puttlitz et al<sup>83</sup> may relate to the use of moment-controlled versus displacement-controlled testing. The relative benefits of each form of testing have been discussed previously in the literature review. For this project displacement-controlled testing was chosen due to availability of a previously validated testing robot.<sup>33</sup> It is possible that different results would be seen for the two forms of testing as insertion of the staple would likely alter the IAR of a segment that was allowed to move freely (i.e. as in moment-controlled testing). Conversely when a fixed IAR was used (i.e. as in displacement-controlled testing) the stiffness of the segment and the strain imparted on the staple for each direction of movement will be a consequence of the relationship between the staple position and the IAR for the plane in which the motion occurs.

In our study we have attempted to create a superior testing methodology. By using only single motion segments and not re-using testing specimens we hope to have minimised confounding factors. In addition, the use of only one staple construct, the double-pronged laterally placed staple, which is the most commonly used clinically, increases the relevance of the findings.

An explanation for the finding of decreased motion segment stiffness may be found in the outcomes of the strain gauge testing and micro-CT scan. The strain gauge testing showed that once inserted the staple tips applied a baseline compressive force to the surrounding trabecular bone and vertebral end-plate. This finding would be consistent with the belief that the mechanism of effect of the SMA staple is via the Hueter-Volkman law. Interestingly however, as the motion segment progressed through the five cycles of each test the baseline load on the staple tips gradually decreased, implying that the force at the staple tip-bone interface was decreasing. We believe that this was likely occurring as a result of structural damage to the trabecular bone and vertebral end-plate by the staple effectively causing 'loosening' of the staple.

This hypothesis is further supported by the findings of the micro-CT scan. The pictures depict significant trabecular bone and physeal injury around the staple blades. Furthermore the staple blades are shown to 'clamp down' once inserted. This position would be unlikely to allow a uniform compressive force on the growth plate for growth modulation and thus poorly reflect the principles of the Hueter-Volkman law and the successful vertebral growth modulation techniques demonstrated in rat models. <sup>68,69,101</sup>

Early results to date with SMA staples have been promising with their effectiveness in creating and then correcting curves in large animal models been shown. <sup>17,21</sup> In addition Betz and colleagues have published medium term follow-up of a group of children treated with SMA stapling which shows promising results. <sup>8,9</sup> We propose however, that the effectiveness that is suggested by this early work is not as a consequence of the Hueter-Volkman effect but rather the insertion of an SMA staple causes vertebral hemiepiphysiodesis and subsequent convex growth arrest.

Convex anterior and posterior growth arrest has been a well-accepted and effective treatment method in patients with congenital spinal deformity, allowing the progression of curves to cease or even reversal of the deformity with subsequent growth. Previously the indications for convex growth arrest have been well described: a pure scoliotic curve without major kyphosis or lordosis; a progressive curve, the magnitude of which is less than 70 degrees; a curve length consisting of five segments or less; patient age less than five years old; no cervical spine involvement and no myelomeningocele; and without a unilateral unsegmented bar as the aetiology of the curve. <sup>105,109,117</sup> However, recently Uzumcugil et al <sup>107</sup> in their review of 32 patients treated with convex growth arrest found that none of the factors can be used to help predict outcome and that the indications for surgery could likely be safely extended.

The published outcomes of convex growth arrest in congenital scoliosis have generally been successful. Roaf reported that 60% of his patients had correction of at least 10°. <sup>87</sup> In the study by Keller et al., 37% of the curves improved, 42% remained unchanged, 16% progressed between 10 and 15°, and only 5% progressed more than 15°. <sup>57</sup> In the study by Winter et al., the curves in five of thirteen patients showed steady improvement over time and a gain of correction of at least 5° beyond that gained by casting, indicating a true epiphysiodesis effect; seven showed cessation of progression of the curve but no improvement over time, indicating a fusion effect; and only one had an increase in deformity, indicating failure. The average correction due to the epiphysiodesis was 10° (range, 5° to 20°). <sup>117</sup> Thompson et al. also had a high success rate. Seventy-six percent of their thirty patients had improvement in the Cobb angle. There was also an average rate of curve improvement of 1.2° per year following the operation, whereas the average worsening prior to the operation had been 1.9°. In their series, there was better improvement in the lumbar curves than in the high thoracic, thoracic, or thoracolumbar curves. <sup>105</sup>

To date no study has evaluated the use of convex growth arrest in idiopathic scoliosis. Based on our findings it is likely that the insertion of an SMA staple causes a similar, albeit somewhat less invasive and extensive, epiphysiodesis effect as has been described for use in congenital scoliosis. The endoscopic insertion of the SMA staple is a significantly less extensive procedure than the traditionally described epiphysiodesis procedures involving partial discectomy, partial resection of the endplate, and posterior decortication. And, although results are early, this doesn't appear to have a significant effect on the outcome as evidenced by the promising early results of Betz et al <sup>8,9,105</sup>, and the early experience at our institution. If an epiphysiodesis effect is not desirable in the treatment of idiopathic scoliosis then alternative staples designs may need to be considered. The screw and plate designs proposed by Wall et al <sup>110</sup> and Schmid et al <sup>93</sup> (see Figure 13) would likely adhere to the principles required for the Hueter-Volkman effect as well as more closely reflecting the uniform compression of the growth plate successfully used in vertebral growth modulation studies in rats. <sup>68,69,103</sup>

A further outcome from this project relating to staple design relates to the material from which it is constructed. As mentioned previously the proposed benefit of constructing the staple from a shape memory alloy is that following insertion the staple should 'clamp' down into the vertebrae to provide secure fixation. Based on the pattern of bone damage on the micro-CT scan it would seem that the staple blades effectively 'cut' downwards into their final resting position as they are hammered in. This finding is supported by examination of the staple tips which have a bevelled edge designed in a fashion to facilitate downwards cutting whilst they are inserted (see Figure 34). Based on this finding it may be that the staple need not be manufactured from a relatively expensive alloy such as nitinol but rather a less expensive material could be used thereby decreasing the cost of the implant.



**Figure 34.** Photograph of an SMA staple. The circle indicates the bevelled staple tip which would facilitate downwards cutting and the staple blade advances forward.

In summary, thoracic SMA stapling is a technique which has shown promising early clinical results. Based on our findings it is likely that the clinical effect is due to vertebral hemiepiphysiodesis causing convex growth arrest. If it is decided that this effect is not desired then alternative staple designs may need to be considered.

## References

1. Adams M, Hutton W. The relevance of torsion to the mechanical derangement of the lumbar spine. *Spine* 1981;6:241-8.
2. Allington NJ, Bowen JR. Adolescent idiopathic scoliosis: treatment with the wilmington brace. A comparison of full-time and part-time use. *J Bone Joint Surg Am* 1996;78:1056-62.
3. Andersen MA, Andersen GR, Thomsen K, et al. Early weaning might reduce the psychological strain of Boston bracing: a study of 136 patients with adolescent idiopathic scoliosis at 3.5 years after termination of brace treatment. *J Pediatr Orthop B* 2002;11:96-9.
4. Arkin AM, Katz JF. The effects of pressure on epiphyseal growth; the mechanism of plasticity of growing bone. *J Bone Joint Surg Am* 1956;38:1056-76.
5. Aronsson DD, Stokes IA, Rosovsky J, et al. Mechanical modulation of calf tail vertebral growth: implications for scoliosis progression. *J Spinal Disord* 1999;12:141-6.
6. Ascani E, Bartolozzi P, Logroscino CA, et al. Natural history of untreated idiopathic scoliosis after skeletal maturity. *Spine* 1986;11:784-9.
7. Bengtsson G, Fallstrom K, Jansson B, et al. A psychological and psychiatric investigation of the adjustment of female scoliosis patients. *Acta Psychiatr Scand* 1974;50:50-9.
8. Betz RR, D'Andrea LP, Mulcahey MJ, et al. Vertebral body stapling procedure for the treatment of scoliosis in the growing child. *Clin Orthop* 2005;55-60.
9. Betz RR, Kim J, D'Andrea LP, et al. An innovative technique of vertebral body stapling for the treatment of patients with adolescent idiopathic scoliosis: a feasibility, safety, and utility study. *Spine* 2003;28:S255-65.
10. Bezzi M, Orsi F, Salvatori FM, et al. Self-expandable nitinol stent for the management of biliary obstruction: long-term clinical results. *J Vasc Interv Radiol* 1994;5:287-93.
11. Bick EM, Copel JW. Longitudinal growth of the human vertebra; a contribution to human osteogeny. *J Bone Joint Surg Am* 1950;32:803-14.
12. Bick EM, Copel JW. The ring apophysis of the human vertebra; contribution to human osteogeny. *J Bone Joint Surg Am* 1951;33:783-7.
13. Birchall D, Hughes D, Gregson B, et al. Demonstration of vertebral and disc mechanical torsion in adolescent idiopathic scoliosis using three-dimensional MR imaging. *Eur Spine J* 2005;14:123-9.
14. Bjerkreim I, Hassan I. Progression in untreated idiopathic scoliosis after end of growth. *Acta Orthop Scand* 1982;53:897-900.
15. Blount WP, Clarke GR. Control of bone growth by epiphyseal stapling: a preliminary report. *J Bone Joint Surg Am* 1949;31:464-78.
16. Bonnel F, Peruchon E, Baldet P, et al. Effects of compression on growth plates in the rabbit. *Acta Orthop Scand* 1983;54:730-3.
17. Braun JT, Akyuz E, Ogilvie JW, et al. The efficacy and integrity of shape memory alloy staples and bone anchors with ligament tethers in the fusionless treatment of experimental scoliosis. *J Bone Joint Surg Am* 2005;87:2038-51.

18. Braun JT, Akyuz E, Udall H, et al. Three-dimensional analysis of 2 fusionless scoliosis treatments: a flexible ligament tether versus a rigid-shape memory alloy staple. *Spine* 2006;31:262-8.
19. Braun JT, Hines JL, Akyuz E, et al. Relative versus absolute modulation of growth in the fusionless treatment of experimental scoliosis. *Spine* 2006;31:1776-82.
20. Braun JT, Hoffman M, Akyuz E, et al. Mechanical modulation of vertebral growth in the fusionless treatment of progressive scoliosis in an experimental model. *Spine* 2006;31:1314-20.
21. Braun JT, Ogilvie JW, Akyuz E, et al. Fusionless scoliosis correction using a shape memory alloy staple in the anterior thoracic spine of the immature goat. *Spine* 2004;29:1980-9.
22. Braun JT, Ogilvie JW, Akyuz E, et al. Experimental scoliosis in an immature goat model: a method that creates idiopathic-type deformity with minimal violation of the spinal elements along the curve. *Spine* 2003;28:2198-203.
23. Brooks HL, Azen SP, Gerberg E, et al. Scoliosis: A prospective epidemiological study. *J Bone Joint Surg Am* 1975;57:968-72.
24. Buehler J, Wang F. A summary of recent research on nitinol alloys and their potential application. *Ocean Engineering* 1968;1:105.
25. Bylski-Austrow DI, Wall EJ, Glos DL, et al. Spinal hemiepiphysiodesis correlates with physal histomorphometric gradients. *Stud Health Technol Inform* 2006;123:261-6.
26. Clayson D, Luz-Alterman S, Cataletto MM, et al. Long-term psychological sequelae of surgically versus nonsurgically treated scoliosis. *Spine* 1987;12:983-6.
27. Climent JM, SÃ¡nchez J. Impact of the type of brace on the quality of life of adolescents with spine deformities. *Spine* 1999;24:1903-8.
28. Cobb J. Outline for the study of scoliosis. In Edwards J ed. *AAOS, Instructional Course Lectures*: Ann Arbor: The American Academy of Orthopedic Surgeons, 1948:261-75.
29. Cotterill PC, Kostuik JP, D'Angelo G, et al. An anatomical comparison of the human and bovine thoracolumbar spine. *J Orthop Res* 1986;4:298-303.
30. Cragg AH, De Jong SC, Barnhart WH, et al. Nitinol intravascular stent: results of preclinical evaluation. *Radiology* 1993;189:775-8.
31. Das K, Rothberg M. Thoracoscopic surgery: historical perspectives. *Neurosurgical Focus* 2000;9:1-3.
32. De Bastiani G, Aldegheri R, Renzi Brivio L, et al. Limb lengthening by distraction of the epiphyseal plate. A comparison of two techniques in the rabbit. *J Bone Joint Surg Br* 1986;68:545-9.
33. de Visser H, Rowe C, Percy M. A robotic testing facility for the measurement of the mechanics of spinal joints. *Proc Inst Mech Eng [H]* 2007;221:221-7.
34. Dickson RA, Lawton JO, Archer IA, et al. The pathogenesis of idiopathic scoliosis. Biplanar spinal asymmetry. *J Bone Joint Surg Br* 1984;66-B:8-15.
35. Edie J, Andreasen G, Zaytoun M. Surface corrosion of nitinol and stainless steel under clinical conditions. *Orthodontics* 1978;54:319-24.

36. Edwards W, Hayes W, Posner I, et al. Variation of lumbar spine stiffness with load. *J Biomech Eng* 1987;109:35-42.
37. Fallstrom K, Cochran T, Nachemson A. Long-term effects on personality development in patients with adolescent idiopathic scoliosis. Influence of type of treatment. *Spine* 1986;11:756-8.
38. Gatehouse SC, Izatt MT, Adam CJ, et al. Perioperative aspects of endoscopic anterior scoliosis surgery: the learning curve for a consecutive series of 100 patients. *J Spinal Disord* 2007;20:317-23.
39. Goel VK, Wilder DG, Pope MH, et al. Biomechanical testing of the spine. Load-controlled versus displacement-controlled analysis. *Spine* 1995;20:2354-7.
40. Gonzalez Barrios I, Fuentes Caparras S, Avila Jurado M. Anterior thoracoscopic epiphysiodesis in the treatment of a crankshaft phenomenon. *Eur Spine J* 1995;4:343-6.
41. Gooding CA, Neuhauser EB. Growth and development of the vertebral body in the presence and absence of normal stress. *Am J Roentgenol* 1965;93:388-94.
42. Goodwin R, James K, Daniels A, et al. Distraction and compression loads enhance spine torsional stiffness. *J Biomech* 1994;27:1049-57.
43. Grassmann S, Oxland T, Gerich U, et al. Constrained testing conditions affect the axial rotation response of lumbar functional spinal units. *Spine* 1998;23:1155-62.
44. Grivas T, Mouzzakis V, Vasiliadis E, et al. Why the prevalence of AIS is different in various countries? Relation to geographic latitude and the possible role of the age of menarche. In Lenke L ed. Proceedings of IMAST. Banff, 2005:Paper 48.
45. Guo X, Chau WW, Chan YL, et al. Relative anterior spinal overgrowth in adolescent idiopathic scoliosis: results of disproportionate endochondral-membranous bone growth. *J Bone Joint Surg Br* 2003;85:1026-31.
46. Guo X, Chau WW, Chan YL, et al. Relative anterior spinal overgrowth in adolescent idiopathic scoliosis-result of disproportionate endochondral-membranous bone growth? Summary of an electronic focus group debate of the IBSE. *Eur Spine J* 2005;14:862-73.
47. Harms J, Jeszenszky D, Beele B. Ventral correction of thoracic scoliosis. In Bridwell K, DeWald R eds. *The Textbook of Spinal Surgery*. 2nd ed. Philadelphia: Lippincott-Raven, 1997:611-26.
48. Hausegger KA, Cragg AH, Lammer J, et al. Iliac artery stent placement: clinical experience with a nitinol stent. *Radiology* 1994;190:199-202.
49. Henry M, Amor M, Beyar R, et al. Clinical Experience with a new nitinol self-expanding stent in peripheral arteries. *J Endovasc Surg* 1996;3:369-79.
50. Hocine L. *Shape memory implants* ed. Berlin: Springer, 2000.
51. Horowitz MB, Moossy JJ, Julian T, et al. Thoracic discectomy using video assisted thoracoscopy. *Spine* 1994;19:1082-6.
52. Hueter C. Anatomische studien an den extremitaetengelenken neugborener und erwachsener. *Virkows Archi Path Anat Physiol* 1862;25:572-99.
53. Izatt MT, Harvey JR, Adam CJ, et al. Recovery of pulmonary function following endoscopic anterior scoliosis correction: evaluation at 3, 6, 12, and 24 months after surgery. *Spine* 2006;31:2469-77.

54. James JI. Idiopathic scoliosis: the prognosis, diagnosis, and operative indications related to curve patterns and the age of onset. *J Bone Joint Surg Br* 1954;36:36-49.
55. Kane WJ, Moe JH. A scoliosis-prevalence survey in Minnesota. *Clin Orthop* 1970;69:216-8.
56. Karol LA. Effectiveness of bracing in male patients with idiopathic scoliosis. *Spine* 2001;26:2001-5.
57. Keller PM, Lindseth RE, DeRosa GP. Progressive congenital scoliosis treatment using a transpedicular anterior and posterior convex hemiepiphysiodesis and hemiarthrodesis. A preliminary report. *Spine* 1994;19:1933-9.
58. Kumar K. Spinal deformity and axial traction. *Spine* 1996;21:653-5.
59. Landreneau RJ, Hazelrigg SR, Mack MJ, et al. Postoperative pain-related morbidity: video-assisted thoracic surgery versus thoracotomy. *Ann Thorac Surg* 1993;56:1285-9.
60. Lindeman M, Behm K. Cognitive strategies and self-esteem as predictors of brace-wear noncompliance in patients with idiopathic scoliosis and kyphosis. *J Pediatr Orthop* 1999;19:493-9.
61. Lonstein J, Bradford D, Winter R, et al. *Moe's Textbook of Scoliosis and Other Spinal Deformities*. 3rd ed. Philadelphia: PA: Saunders, 1995.
62. Lonstein JE, Carlson JM. The prediction of curve progression in untreated idiopathic scoliosis during growth. *J Bone Joint Surg Am* 1984;66:1061-71.
63. Mack MJ, Regan JJ, Bobechko WP, et al. Application of thoracoscopy for diseases of the spine. *Ann Thorac Surg* 1993;56:736-8.
64. MacLean WE, Green NE, Pierre CB, et al. Stress and coping with scoliosis: psychological effects on adolescents and their families. *J Pediatr Orthop* 1989;9:257-61.
65. McAfee PC, Regan JR, Zdeblick T, et al. The incidence of complications in endoscopic anterior thoracolumbar spinal reconstructive surgery. A prospective multicenter study comprising the first 100 consecutive cases. *Spine* 1995;20:1624-32.
66. McCall IW, Galvin E, O'Brien JP, et al. Alterations in vertebral growth following prolonged plaster immobilisation. *Acta Orthop Scand* 1981;52:327-30.
67. Medtronic. SMA Staple - Surgical Technique.
68. Mente PL, Aronsson DD, Stokes IA, et al. Mechanical modulation of growth for the correction of vertebral wedge deformities. *J Orthop Res* 1999;17:518-24.
69. Mente PL, Stokes IA, Spence H, et al. Progression of vertebral wedging in an asymmetrically loaded rat tail model. *Spine* 1997;22:1292-6.
70. Miller NH. Genetics of familial idiopathic scoliosis. *Clin Orthop* 2007;462:6-10.
71. Nachemson AL, Peterson LE. Effectiveness of treatment with a brace in girls who have adolescent idiopathic scoliosis. A prospective, controlled study based on data from the brace study of the scoliosis research society. *J Bone Joint Surg Am* 1995;77:815-22.
72. Nachlas IW, Borden JN. The cure of experimental scoliosis by directed growth control. *J Bone Joint Surg Am* 1951;33:24-34.

73. Newton PO, Farnsworth CL, Faro FD, et al. Spinal growth modulation with an anterolateral flexible tether in an immature bovine model: disc health and motion preservation. *Spine* 2008;33:724-33.
74. Newton PO, Faro FD, Farnsworth CL, et al. Multilevel spinal growth modulation with an anterolateral flexible tether in an immature bovine model. *Spine* 2005;30:2608-13.
75. Noonan KJ, Dolan LA, Jacobson WC, et al. Long-term psychosocial characteristics of patients treated for idiopathic scoliosis. *J Pediatr Orthop* 1997;17:712-7.
76. Panjabi MM. Biomechanical evaluation of spinal fixation devices: I. A conceptual framework. *Spine* 1988;13:1129-34.
77. Panjabi MM, Brand RA, White AA. Mechanical properties of the human thoracic spine as shown by three-dimensional load-displacement curves. *J Bone Joint Surg Am* 1976;58:642-52.
78. Panjabi MM, Brand RA, White AA. Three-dimensional flexibility and stiffness properties of the human thoracic spine. *J Biomech* 1976;9:185-92.
79. Parent S, Labelle H, Skalli W, et al. Vertebral wedging characteristic changes in scoliotic spines. *Spine* 2004;29:E455-62.
80. Parent S, Labelle H, Skalli W, et al. Morphometric analysis of anatomic scoliotic specimens. *Spine* 2002;27:2305-11.
81. Perdriolle R, Becchetti S, Vidal J, et al. Mechanical process and growth cartilages. Essential factors in the progression of scoliosis. *Spine* 1993;18:343-9.
82. Peterson LE, Nachemson AL. Prediction of progression of the curve in girls who have adolescent idiopathic scoliosis of moderate severity. Logistic regression analysis based on data from the brace study of the scoliosis research society. *J Bone Joint Surg Am* 1995;77:823-7.
83. Puttlitz CM, Masaru F, Barkley A, et al. A biomechanical assessment of thoracic spine stapling. *Spine* 2007;32:766-71.
84. Riley LH, Eck JC, Yoshida H, et al. A biomechanical comparison of calf versus cadaver lumbar spine models. *Spine* 2004;29:E217-20.
85. Riseborough EJ, Wynne-Davies R. A genetic survey of idiopathic scoliosis in Boston, Massachusetts. *J Bone Joint Surg Am* 1973;55:974-82.
86. Roaf R. Vertebral growth and its mechanical control. *J Bone Joint Surg Br* 1960;42-B:40-59.
87. Roaf R. The treatment of progressive scoliosis by unilateral growth arrest. *J Bone Joint Surg Br* 1963;45-B:637-51.
88. Roaf R. The basic anatomy of scoliosis. *J Bone Joint Surg Br* 1966;48-B:786-92.
89. Rosenthal D, Marquardt G, Lorenz R, et al. Anterior decompression and stabilization using a microsurgical endoscopic technique for metastatic tumors of the thoracic spine. *J Neurosurg* 1996;84:565-72.
90. Rowe DE, Bernstein SM, Riddick MF, et al. A meta-analysis of the efficacy of non-operative treatments for idiopathic scoliosis. *J Bone Joint Surg Am* 1997;79:664-74.
91. Ryhanen J, Kallioinen M, Tuukkanen J, et al. In vivo biocompatibility evaluation of nickel-titanium shape memory metal alloy: Muscle and perineural

- tissue responses and capsule membrane thickness. *J Biomed Mater Res* 1998;41:481-8.
92. Sanders JO, Sanders AE, More R, et al. A preliminary investigation of shape memory alloys in the surgical correction of scoliosis. *Spine* 1993;18:1640-6.
  93. Schmid EC, Aubin C, Moreau A, et al. A novel fusionless vertebral physal device inducing spinal growth modulation for the correction of spinal deformities. *Eur Spine J* 2008;17:1329-35.
  94. Schwaninger B, Sarcar N, Foster B. Effects of long term immersion on the flexural properties of nitinol. *Am J Orthod* 1982;182:45-9.
  95. Scoles PV, Latimer BM, Digiovanni BF, et al. Vertebral alterations in Scheuermann's kyphosis. *Spine* 1991;16:509-15.
  96. Smith AD, Von Lackum WH, Wylie R. An operation for stapling vertebral bodies in congenital scoliosis. *J Bone Joint Surg Am* 1954;36:342-8.
  97. Somerville EW. Rotational lordosis: the development of the single curve. *J Bone Joint Surg Br* 1952;34-B:421-7.
  98. Staheli LT. *Fundamentals of pediatric orthopedics*. 3rd ed. Philadelphia: Lippincott Williams & Wilkins, 2003.
  99. Stokes IA. Three-dimensional terminology of spinal deformity. A report presented to the Scoliosis Research Society by the Scoliosis Research Society Working Group on 3-D terminology of spinal deformity. *Spine* 1994;19:236-48.
  100. Stokes IA, Aronsson DD, Urban JPG. Biomechanical factors influencing progression of angular skeletal deformities during growth. *Eur J Exp Musculoskeletal Res* 1994;3:51-60.
  101. Stokes IA, Spence H, Aronsson DD, et al. Mechanical modulation of vertebral body growth. Implications for scoliosis progression. *Spine* 1996;21:1162-7.
  102. Stokes IAF. Mechanical modulation of spinal growth and progression of adolescent scoliosis. *Stud Health Technol Inform* 2008;135:75-83.
  103. Stokes IAF, Aronsson DD, Dimock AN, et al. Endochondral growth in growth plates of three species at two anatomical locations modulated by mechanical compression and tension. *J Orthop Res* 2006;24:1327-34.
  104. Swartz DE, Wittenberg RH, Shea M, et al. Physical and mechanical properties of calf lumbosacral trabecular bone. *J Biomech* 1991;24:1059-68.
  105. Thompson AG, Marks DS, Sayampanathan SR, et al. Long-term results of combined anterior and posterior convex epiphysiodesis for congenital scoliosis due to hemivertebrae. *Spine* 1995;20:1380-5.
  106. Unkown. Patient information: gentle guided growth to correct knock knees and bowed legs in children: Orthofix, 2007.
  107. Uzumcugil A, Cil A, Yazici M, et al. Convex growth arrest in the treatment of congenital spinal deformities, revisited. *J Pediatr Orthop* 2004;24:658-66.
  108. Volkmann R. Verletzungen und krankheiten der bewegungsorgane. In Billroth c ed. *Handbuch der allgemeinen und speciellen chirurgie, Bd II, Teil II*. Stuttgart: Ferdinand Enke, 1882.
  109. Walhout R, van Rhijn L, Pruijs J. Hemi-epiphysiodesis for unclassified congenital scoliosis: immediate results and mid-term follow-up. *Eur Spine J* 2002;11:543-9.

110. Wall EJ, Bylski-Austrow DI, Kolata RJ, et al. Endoscopic mechanical spinal hemiepiphysiodesis modifies spine growth. *Spine* 2005;30:1148-53.
111. Weinstein S. *The Pediatric Spine: Principles and Practice* ed. New York: NY: Raven Press, Ltd, 1994.
112. Weinstein SL, Ponseti IV. Curve progression in idiopathic scoliosis. *J Bone Joint Surg Am* 1983;65:447-55.
113. Wever, Wever D, Elstrodt, et al. Scoliosis correction with shape-memory metal: results of an experimental study. *Eur Spine J* 2002;11:100-6.
114. Wever DJ, Veldhuizen AG, Sanders MM, et al. Cytotoxic, allergic and genotoxic activity of a nickel-titanium alloy. *Biomaterials* 1997;18:1115-20.
115. Wilke HJ, Krischak S, Claes L. Biomechanical comparison of calf and human spines. *J Orthop Res* 1996;14:500-3.
116. Wilke HJ, Krischak ST, Wenger KH, et al. Load-displacement properties of the thoracolumbar calf spine: experimental results and comparison to known human data. *Eur Spine J* 1997;6:129-37.
117. Winter RB, Lonstein JE, Denis F, et al. Convex growth arrest for progressive congenital scoliosis due to hemivertebrae. *J Pediatr Orthop* 1988;8:633-8.
118. Xiong B, Sevastik JA, Hedlund R, et al. Radiographic changes at the coronal plane in early scoliosis. *Spine* 1994;19:159-64.

## APPENDIX 1. EFFECT OF TEMPERATURE ON STAPLE STIFFNESS

### Methods

1. A rig was created by machining two screws, which were clamped into a Hounsfield tensile testing machine with a load cell of 500N.
2. Provision was made to control the temperature of the staple by using a plastic cup, sealed with clay, of sufficient size to allow complete immersion of the staple.
3. A water bath was obtained and maintained at 37°C
4. All tests displaced the staple 2 millimetres over 30 seconds, and unloaded the staple in the same manner. This loading\unloading cycle was repeated 5 times. The staple was initially unloaded. The resulting force was measured and recorded.
5. The following tests were performed:
  - a. Room temperature tests with no fluid in the rig
  - b. Room temperature tests with fluid in the rig
  - c. 37°C tests after bathing the staple in the heated water bath for several minutes, and heated water placed in the rig. The temperature was measured at the conclusion of the 5 tests.
6. These three tests were repeated, with the only difference being the heated water was continuously run over the sample.
7. The loading\unloading curve was assessed for linearity and hysteresis and compared with similar known nitinol curves.
8. The stiffness (in N/mm) of the staple upon loading was estimated at different temperatures. Data points were considered admissible if they contained force values >0.1N. These stiffnesses were compared for significance.

**Results: Summary of stiffness at measured temperatures**

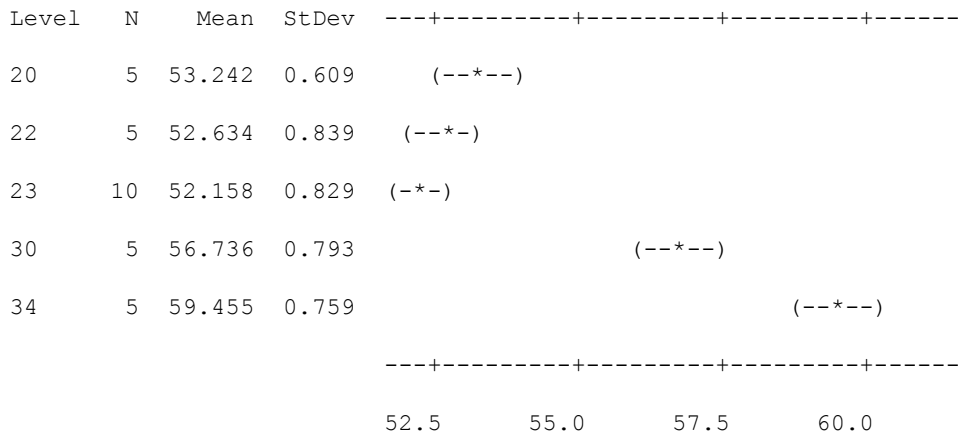
Temperature	Bathed in Fluid	Average Stiffness (N/mm)	Minimum R <sup>2</sup> Value
23	N	51.76	0.983
23	N	52.56	0.980
20	Y	53.24	0.981
22	Y	52.63	0.979
37-30	Y	56.74	0.990
37-34	Y	59.46	0.991

**One-way ANOVA: Slope versus End Temperature**

Source	DF	SS	MS	F	P
End Temperature	4	227.626	56.906	92.96	0.000
Error	25	15.304	0.612		
Total	29	242.930			

S = 0.7824 R-Sq = 93.70% R-Sq(adj) = 92.69%

Individual 95% CIs For Mean Based on  
Pooled StDev



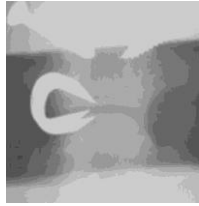
Pooled StDev = 0.782

### Conclusion

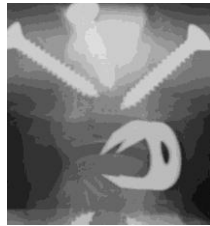
There is a significant difference between the tests conducted at 20-23°C and those conducted at 37-30°C. This difference is approximately 5.5 N/mm, representing around 9% of the total stiffness. No significant difference was found due to the use of the water bath.

## APPENDIX 2. POST-TEST X-RAYS CONFIRMING STAPLE POSITION

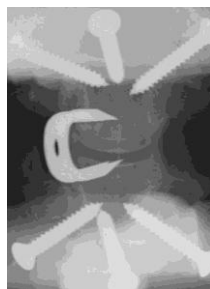
**Test 1**



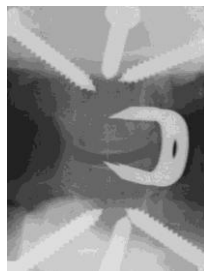
**Test 2**



**Test 3**



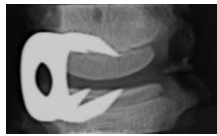
**Test 4**



**Test 5**



**Test 6**



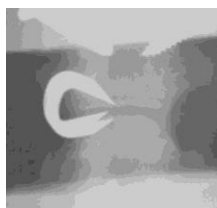
**Test 7**



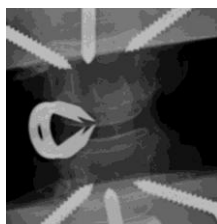
**Test 8**



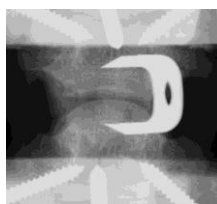
**Test 9**



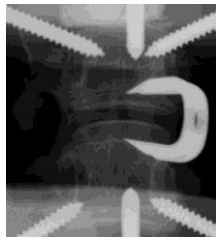
**Test 10**



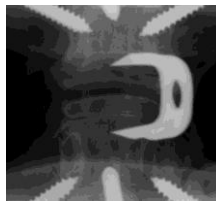
**Test 11**



**Test 12**



**Test 13**



**Test 14**

